LAJSBA
LATIN AMERICAN JOURNAL OF SEDIMENTOLOGY AND BASIN ANALYSIS | VOLUME 32 (2) 2025, 168-191

MICROFACIES TEXTURAL VARIABILITY IN FLUVIO-AEOLIAN SANDSTONES FROM THE AVILÉ MEMBER, NEUQUÉN BASIN, ARGENTINA

Eusebio Coelho Tenazinha[1*], *Joaquín Pérez Mayoral*[1], *Gonzalo D. Veiga*[1]

[1] Centro de Investigaciones Geológicas, Consejo Nacional de Investigaciones Científicas y Técnicas (CONICET) – Universidad Nacional de La Plata (UNLP). Diagonal 113 #275, La Plata, Argentina.
*Corresponding author: ecoelho@cig.museo.unlp.edu.ar

ARTICLE INFO

Article history
Received March 3, 2025
Accepted December 5, 2025
Available online December 19, 2025

Handling Editor
Giorgio Basilici

Keywords
Aeolian microfacies
Fluvial microfacies
Grain size analysis
Petrographic characterisation
Textural parameters

ABSTRACT

Understanding the internal microtextural heterogeneity of fluvio-aeolian successions can provide valuable insights both on the depositional mechanisms associated with their origin and on their quality as reservoir rocks. Microfacies analysis enables the integration of thin-section textural studies with outcrop-scale observations, which substantially improves our understanding of depositional dynamics across different subenvironments, as well as the interpretation of petrophysical properties distribution. This approach is particularly relevant for reservoirs such as the Avilé Member of the Agrio Formation, as small-scale textural variability has become increasingly important due to the implementation of enhanced recovery techniques in recent years. This unit is characterised by fluvial and aeolian sandstones and constitutes one of the main conventional hydrocarbon reservoirs in the Neuquén Basin. In light of this, the general objective of this work was to compare aeolian and fluvial laminae to improve small-scale textural heterogeneities modelling of the defined facies from mesoscopic analysis. The methodology involved first describing and interpreting the units at the mesoscopic scale, and then characterising the different lamina types at the microscopic scale to define the microfacies. Five distinct lamina types, each representing a specific sedimentary process, were identified in the field within a well-established stratigraphic framework. Their textural petrographic characterisation allowed the definition of five corresponding microfacies —three associated with aeolian deposits and two with fluvial deposits. The results suggest a strong correspondence between textural parameters and the sedimentary process responsible for deposition. The analysis showed both differences among deposits formed by the same transport and depositional agent, and similarities between aeolian and fluvial deposits formed by analogous depositional mechanisms. This suggests that the depositional process may exert greater control on deposit texture than the characteristics of the transport and depositional agent. The study contributes to a more accurate characterisation of small-scale heterogeneities, which is essential for improving facies modelling and reservoir prediction. Overall, the findings highlight the complexity of interpreting microtextural heterogeneity and underscore the value of detailed microfacies analysis as a complement to field studies for improved reservoir characterisation.

INTRODUCTION

Fluvio-aeolian successions are known to constitute some of the most important conventional hydrocarbon reservoirs worldwide and typically exhibit textural heterogeneity at various scales (Mountney, 2006; Al-Masrahy and Mountney, 2014; Rodríguez-López *et al.*, 2014). At the microscopic level, the study of this heterogeneity can be approached through the determination of grain size and fabric parameters to define microfacies or microfabrics (Limarino *et al.*, 2015). These features are key components of clastic texture, a property that largely reflects the depositional process(es) of the rock (Tucker, 2001), and both exert a strong influence on their physical properties, such as porosity, permeability and bulk density (Tucker and Jones, 2023). Microfacies analysis thus enables the study of specific transport and depositional mechanisms related to their origin, as well as the interpretation of subtle variations in petrophysical properties of the rocks (Limarino *et al.*, 2015). A key aspect of aeolian and fluvial sandstone deposits when they are found together is that they are commonly composed of diverse fine-scale laminated lithologies. The role these laminations play in controlling capillary trapping within a reservoir is then important to consider, especially when the presence of strong permeability contrasts between laminae can significantly influence multiphase flow behaviour that must be properly represented in reservoir models (Bentley and Ringrose, 2021).

In general terms, distinctive textural and petrophysical characteristics are exhibited by aeolian and fluvial deposits (Robinson, 1981; Fryberger *et al.*, 2011; Jarzyna *et al.*, 2009; Bofill *et al.*, 2025). Variations in porosity and permeability between aeolian and fluvial sandstones have been studied in detail, especially in one of the major hydrocarbon reservoirs from North Sea Basin (the Permian Rotliegend Sandstone, UK and the Netherlands; Fryberger *et al.*, 2011). Fryberger *et al.* (2011) and Robinson (1981) pointed that aeolian dune sandstones might constitute better hydrocarbon reservoirs than the associated fluvial sandstones due to bulk differences in core porosity and core permeability at regional level. Jarzyna *et al.* (2009) also showed that aeolian dune deposits (Rotliegend Group, Poland) associated with grainflow and grainfall processes might have similar petrophysical properties as fluvial channel sandstones, contrasting with those associated to wind-ripple lamination that had intermediate properties and those to distal fluvial deposits which had the worst reservoir conditions. Lastly, Bofill *et al.* (2025) applied outcrop-based facies analysis (upper section of the Lower Grès Formation, France) to demonstrate that grainfall and grainflow deposits, both aeolian and fluvial, exhibit higher permeability that wind-ripple laminae.

Outcrop-based studies can provide key information for reservoirs under development stages or used for gas storage such as helping to decipher the architectural complexity or understanding how grain arrangement, beyond mere grain size, can affect the petrophysical properties of the rocks. However, macroscopic-scale evidence alone is insufficient to fully understand the sedimentary systems as a whole when it comes to textural features (Limarino *et al.*, 2025). Understanding microscale textural variations —and the processes that produce them— is crucial for predicting petrophysical changes, and associating these predictions with specific facies enables extrapolation to larger scales. In this sense, microfacies studies —underdeveloped to date— enable the integration of thin-section textural analysis with outcrop-scale observations, which substantially improves our understanding of depositional dynamics across different subenvironments, as well as the interpretation of petrophysical properties of the rocks (Limarino *et al.*, 2025). This latter aspect is particularly relevant in advanced stages of reservoir development, where identifying fluid migration pathways and recognising subtle permeability barriers is essential (Limarino *et al.*, 2015). Within this framework, the petrology of sedimentary rocks provides geological insights through valuable tools whose potential has not yet been fully realised.

The multiscale approach described is especially pertinent for units such as the Avilé Member of the Agrio Formation, since it is characterised by a complex interaction between fluvial and aeolian processes (Veiga *et al.*, 2002) and represents a significant hydrocarbon reservoir in the Neuquén Basin (Gulisano *et al.*, 2001; Rossi and Masarik, 2002; Argüello, 2011; Argüello Scotti *et al.*, 2022). With the recent implementation of enhanced recovery techniques, detailed lamina-scale textural analysis has become essential due to the importance of understanding internal microtextural heterogeneity. In light of this, the general objective of this work is

to compare between aeolian and fluvial microfacies to improve small-scale textural heterogeneities modelling of the defined facies from mesoscopic analysis. The specific aims for this work are: i) to describe microfacies of laminae from different genesis within the context of the studied stratigraphic framework, ii) to analyse and explain the differences between distinct microfacies considering the specific sedimentary processes associated with their origin, and iii) to examine the applicability of microfacies analysis in reservoir characterisation.

GEOLOGICAL SETTING

The Neuquén Basin is located in west-central Argentina and comprises a stratigraphic record from the Upper Triassic to the Paleogene (Legarreta and Gulisano, 1989). It is bounded by the Sierra Pintada System to the northeast, the Nordpatagonian Massif to the southeast, and the Andean Volcanic Arc to the west (Fig. 1a). The sedimentary record of the basin was controlled by a combination of eustatic oscillations and a complex tectonic history (Vergani *et al.*, 1995), related to the dynamics of the proto-Andean margin and intraplate activity associated with the breakup of the Gondwana supercontinent (Howell *et al.*, 2005). During the sedimentation of the Mesozoic fill, several continental successions were abruptly deposited over both shallow and deep marine deposits across large-scale unconformities (Leanza, 2009). These deposits have been interpreted as second-order lowstand wedges developed during relative sea-level falls (Legarreta and Gulisano, 1989; Legarreta and Uliana, 1991; Spalletti and Veiga, 2007), enhanced by localised tectonic inversions (Howell *et al.*, 2005).

One of these lowstand wedges is the Avilé Member of the Agrio Formation (Fig. 1b), a lithostratigraphic unit of Hauterivian age (Lower Cretaceous), widely distributed across the central sector of the Neuquén Basin (northern Neuquén and southern Mendoza). It is dominated by the accumulation of fluvial, aeolian and lacustrine deposits (Veiga *et al.*, 2002, 2007, 2011; Prámparo and Veiga, 2024). The unit is described as a thin, extensive wedge whose thickness varies from a few metres in the south to more than 180 metres in northern Neuquén (Veiga *et al.*, 2011). It overlies shallow to deep marine deposits of the Pilmatué Member, which contain fossils of the nominal species of the Weavericeras vacaensis Zone (upper Lower Hauterivian), and underlies deep marine deposits of the Agua de la Mula Member, which bear fossils of the nominal species of the Spitidiscus ricardii Zone (lower Upper Hauterivian; Aguirre Urreta and Rawson, 1997; Aguirre Urreta *et al.*, 2005).

The Avilé Member is mainly composed of sandstones and has been one the main conventional hydrocarbon reservoir from the Neuquén Basin, especially in Puesto Hernandez and Chihuido de la Sierra Negra oil fields (Valenzuela *et al.*, 2002; Argüello, 2011; Valenzuela *et al.*, 2011). Drilling of infill wells and waterflood recovery have been performed with success since the late 80's and early 90's and more recently Enhanced Oil Recovery (EOR) pilots have been implemented (Argüello Scotti *et al.*, 2022). Based on facies associations and architectural analysis, Veiga *et al.* (2011) described five depositional systems within the Avilé Member: sandy braided fluvial, mixed-loaded meandering fluvial, aeolian, open lacustrine and hypersaline lacustrine. The distribution and sedimentological characteristics of the unit in north-central Neuquén and southern Mendoza exhibit notable variations in relation to the prevailing accumulation conditions and the depositional systems represented. Consequently, four distinct sectors have been delineated for the Avilé Member, based on the identification of specific depositional features and the lateral and vertical distribution of facies associations, with the northeastern sector being dominated by sandstones and recording fluvial-aeolian interactions (Veiga *et al.*, 2011; Fig. 1c).

DATASET AND METHODS

The study area of the present work corresponds to the Northeastern Sector as defined by Veiga *et al.* (2011), specifically the localities of San Eduardo and Pampa Tril (Fig. 1c). Fieldwork consisted of mesoscopic description of the facies and the collection of 14 oriented samples (11 from San Eduardo and 3 from Pampa Tril). Sampling was facies-driven, aiming to obtain laminae representative of the studied units (aeolian grainflow laminae, aeolian grainfall laminae, wind-ripple laminae, subaqueous grainflow/grainfall laminae, and subaqueous-ripple laminae). Subsequently, 14 thin sections were prepared perpendicular to the lamination, and grain size and fabric were described for each type of lamina in a petrographic microscope. The term

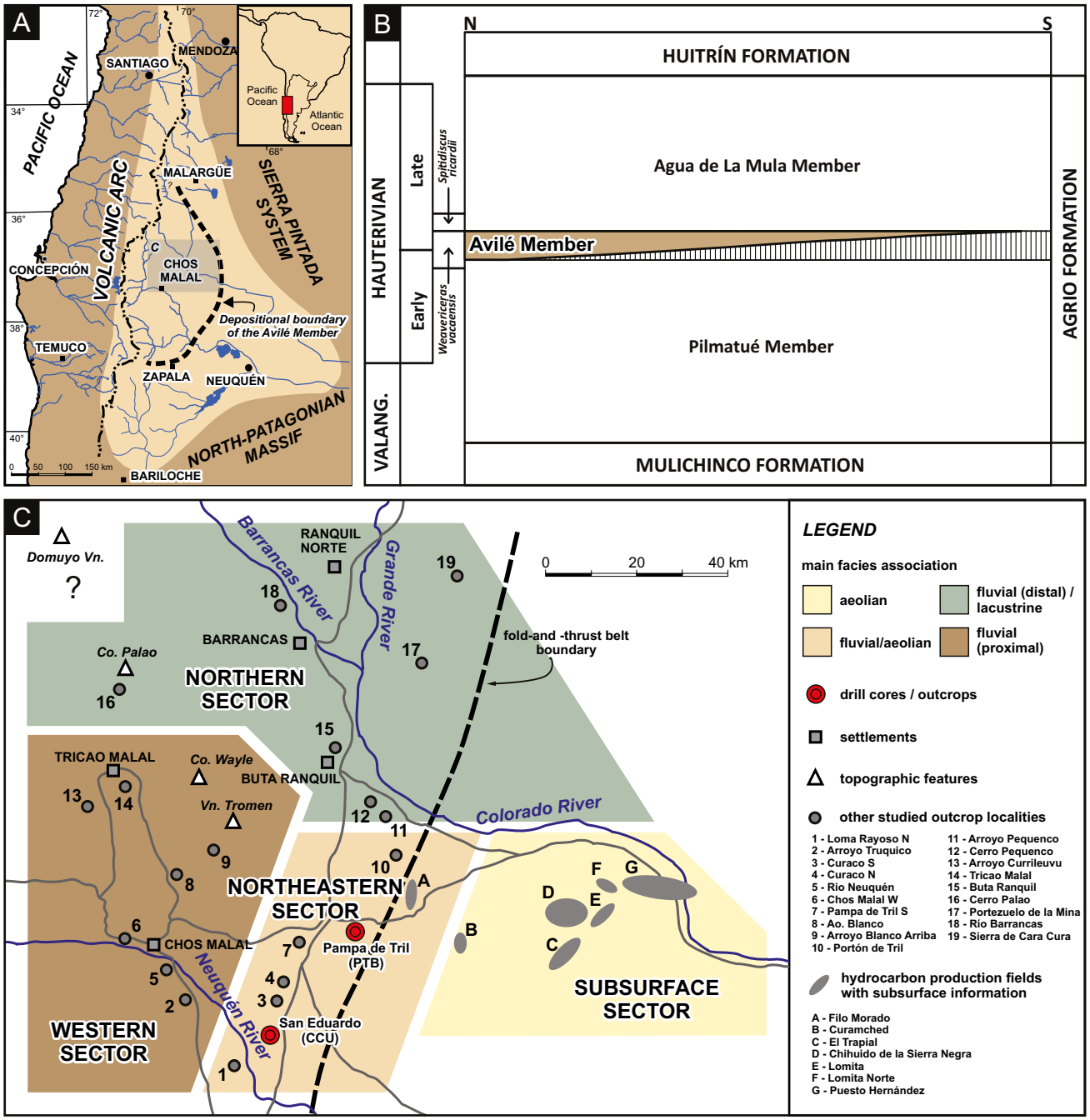

Figure 1. a) Location and limits of the Neuquén Basin (modified from Howell *et al.*, 2005). **b)** Chronostratigraphic chart of the Avilé Member (modified from Veiga *et al.*, 2011). **c)** Location of the Northeastern Sector and the San Eduardo and Pampa Tril localities (modified from Prámparo and Veiga, 2024).

"lamina" used here refers to the finest recognisable layer without internal stratification (Bokman, 1956; Campbell, 1967), with laminae of the same type being those whose origin is associated with the same sedimentary process. Each of the thin sections studied consists of laminae of the same type, except for three cases where the thin sections are composed of alternating laminae of different origins.

To analyse these thin sections, a ZEISS ZEN petrographic microscope was used to visualize, describe, and capture images, which were later analysed using the JMicroVision v1.3.4 program (Roduit, 2022). Using the Point Counting tool, this software allowed random selection of around 450 clastic components for each lamina type present in each of the studied thin sections (Fig. 2a). The components selected through this method were

manually outlined using the 2D Measurement option (Fig. 2b), and the resulting polygons were subsequently converted into classes using the Object Extraction tool (Fig. 2c). As a result, various sets of quantitative attributes that characterise the grain size and shape of the clastic components of the different lamina types in each thin section were automatically generated. Among these attributes, the apparent major axis length (Fig. 2d) was selected as representative of the grain size of the components (Rosenfeld *et al.*, 1953; Friedman, 1958). Then, the corresponding data sets were individually subjected to statistical analysis using Microsoft Office Excel and MATLAB (The MathWorks Inc., 2022). The data processing involved the determination of parameters such as mode, median, mean, standard deviation, skewness, and kurtosis, in accordance with the set of formulas and boundary values proposed by Folk and Ward (1957).

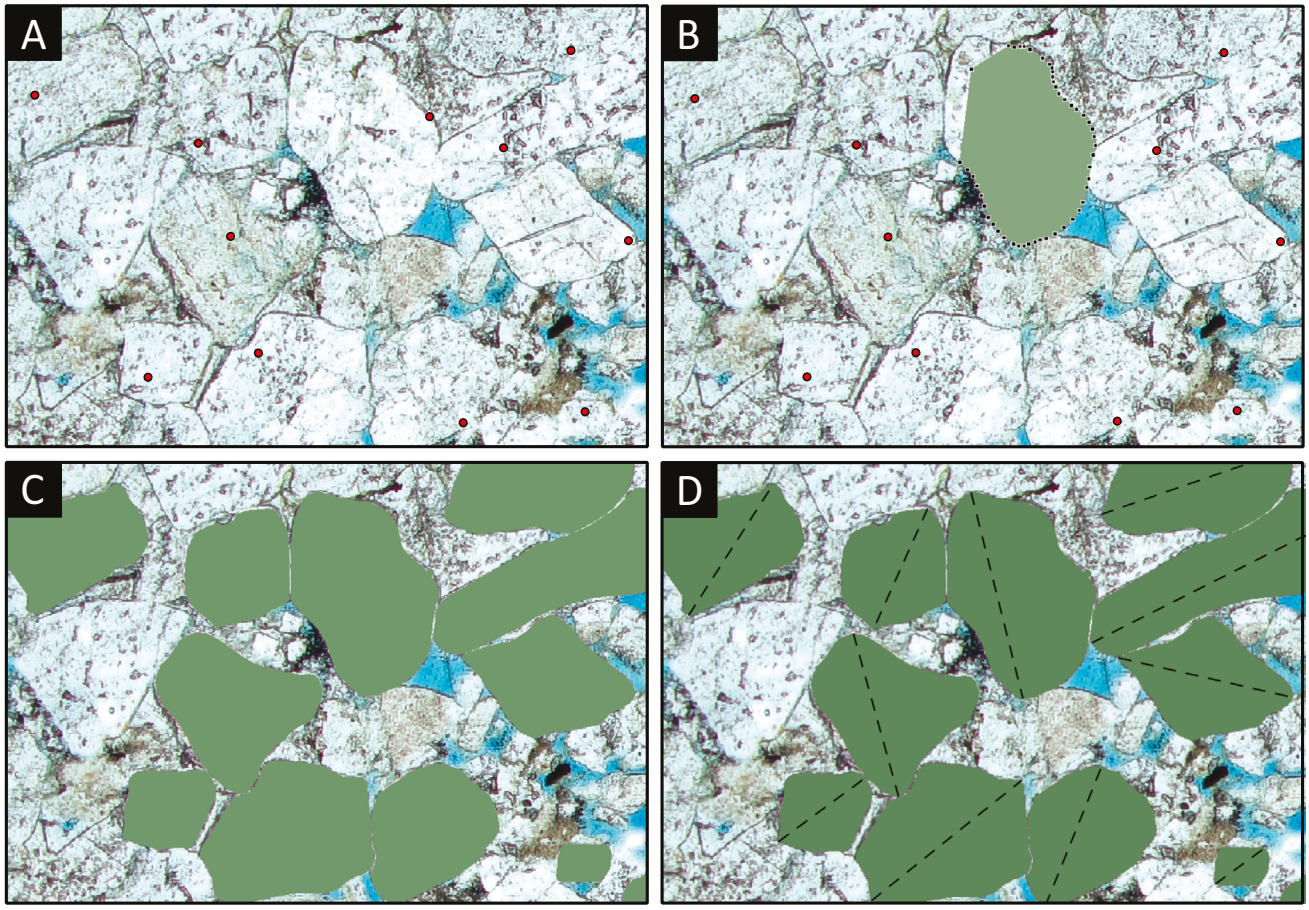

Figure 2. Grain selection and measurement workflow using JMicroVision. **a)** Selection of clasts to be measured through the generation of random points by the Point Counting tool (notice the red points). **b)** Manual contouring of previously selected clasts through 2D Measurement tool. **c)** Conversion of polygons into classes through the Object Extraction option for automatic data generation. **d)** Measurement of the apparent major axis length of each clastic component.

The grain size information was integrated with data related to the fabric of the studied rocks. Fabric refers to the spatial relationships between the components that constitute a sedimentary rock, encompassing the study of fabric heterogeneity (microstructures), clast orientation, and packing (Scasso and Limarino, 1997). The fabric heterogeneity or microstructure was defined qualitatively through microscopic observation and refers to the existence of two or more fabric patterns generally resulting from the textural segregation of particles during transport and deposition (Scasso and Limarino, 1997). Moreover, in relation to packing, defined as the efficient use of space by the mutual arrangement of grains in an aggregate (Pandalai and Basumallick, 1984), the type of

contacts between grains was defined according to Taylor (1950) and the packing proximity index (PPI) was calculated according to Kahn (1956). The latter characterises packing semi-quantitatively and is the percentage ratio between the number of grain-to-grain contacts and the total number of contacts (including grain-to-grain, grain-to-matrix, grain-to-cement, and grain-to-pore contacts) observed along a line, which in this study was positioned parallel to the lamination.

The methods described above enabled the microtextural characterisation of the five lamina types identified in the studied deposits, leading to the definition of five distinct microfacies. These microfacies were subsequently compared based on their textural attributes. For this work, a microfacies is a complementary unit to lithofacies, whose petrographic characteristics related to textural properties reflect the small-scale transport and depositional mechanisms responsible for its formation (Limarino *et al.*, 2025). The concept of microfacies was previously approached by Limarino *et al.* (2015) using the term "microfabric". For the purpose of this analysis, the term microfacies is preferred over microfabrics, as its definition encompasses not only fabric-related information but also grain size. The microfacies analysis can enable the interpretation of changes in the petrophysical properties of rocks (Limarino *et al.*, 2015). However, it should be noted that the influence of diagenetic processes should be considered when characterising microfacies, as mechanical and chemical compaction can alter grain size and, more importantly, the fabric of sedimentary deposits. In the studied laminae, the degree of diagenesis is sufficiently low not to compromise the analysis, although quantifying the diagenetic features could provide a more precise characterisation, especially if the results presented here are to be used to infer petrophysical properties.

MESOSCOPIC ANALYSIS

The record of the Avilé Member in the Pampa Tril and San Eduardo localities results from an intricate interaction between fluvial and aeolian processes that constitute a complex architectural framework as a consequence of the contraction and expansion of the erg system that existed in the central Neuquén Basin during Hauterivian times (Veiga *et al.*, 2002).

Four sedimentary units were defined for the Avilé Member in these localities, based on their outcrop-scale geometry, main lithology, primary sedimentary structures and their constituent laminae (Table 1, Fig. 3). While the most abundant units correspond to aeolian dune and sand sheet deposits (Fig. 4a-c), fluvial channelised sandstones are also prominent, particularly in the San Eduardo locality (Fig. 4d) and in the upper portions of the succession at the Pampa Tril locality. The least common unit is linked to distal fluvial floods (Fig. 4e).

Aeolian dune

Description. Tabular bodies with sharp, horizontal upper and lower boundaries, composed of fine- to very fine-grained, well-sorted sandstones arranged in planar to tangential cross-stratified sets. Thickness ranges from 0.5 to 6 m, and width reaches hundreds of metres. The top portions of the sets have two types of laminae dipping between 20° and 25°: (i) thick, wedge-shaped, inversely graded or massive laminae with coarser grains, and (ii) thin, tabular, massive laminae composed of finer grains. Conversely, at the basal portions of these sets, relatively horizontal, inversely graded regular in thickness bimodal laminae are also recorded.

Interpretation. The upper parts of the sets are interpreted as the result of grainflow and grainfall deposition, respectively, on the steep lee slopes of aeolian bedforms (Hunter, 1977). Grainflows are produced by the reworking of previously accumulated grains, triggered by periodic slope instability when sand locally exceeds its angle of repose, typically at dune crests (Hunter, 1977; Howell and Mountney, 2001). While grainfall deposits originate in flow separation zones, where the airflow detaches from the surface —commonly on the lee side of dune crests (Hunter, 1977); in these zones, finer grains transported by saltation settle preferentially on the upper lee slope as a result of flow deceleration and reduced wind velocity past the crest (Nickling *et al.*, 2002). On the other hand, the lower parts of sets that have relatively horizontal, bimodal, inversely graded laminae are interpreted as wind-ripple lamination, mainly of the subcritically climbing translatent type, located typically at the dune toe (Hunter, 1977; Mountney,

Sedimentary unit	Litology and sedimentary structures	Geometry and dimensions	Sandy laminae description	Interpretation	Studied samples
Aeolian dune	Fine- to medium-grained sandstones arranged in cross-stratified sets	Tabular shaped. 0.5 to 6 m thick. 100s m wide. Sharp horizontal upper and lower boundaries	Set top: thick, wedge-shaped, coarser, inversely graded or massive laminae, and thin, tabular, finer, massive laminae. Set base: horizontal, inversely graded bimodal laminae	Aeolian grainflow and grainfall laminae (set top) and wind-ripple laminae (set base) linked to migration of aeolian dunes	SE-3, SE-7 and PT-1 (grainflow-grainfall laminae); SE-4, SE-5 and SE-8 (wind ripple laminae)
Aeolian sand sheet	Fine- to medium- grained sandstones with horizontal lamination	Tabular shaped. 1 to 2 m thick. 100s m wide. Sharp horizontal upper and lower boundaries	Horizontal, inversely graded bimodal laminae	Wind-ripple laminae linked to aeolian accumulation in sand sheets	SE-2, SE-6 and PT-3 (wind ripple laminae)
Fluvial channels	Medium-grained sandstones arranged in trough cross-stratified sets, and thin, massive layers of rip-up clast conglomerates	Lenticular shaped. Up to 3 m thick. 5 m to 10s m wide. Erosional lower boundaries; flat and sharp upper boundaries	The trough cross-bedded sandstones upper parts are composed by thick, massive laminae	Subaqueous grainfall/ grainflow laminae associated to migration of subaqueous dunes during unidirectional currents	SE-1, SE-9, SE-10 and SE-11 (grainfall/ grainflow laminae)
Distal fluvial floods	Fine-grained sandstones with massive or asymmetrical cross-lamination. Silstones and mudstones with horizontal lamination	Tabular to wedge shaped. Up to 4 m thick. 100s m wide. Sharp and horizontal upper and lower boundaries	Fine, massive or asymmetrical cross-laminae	Combination of ponded water accumulation and repeated flooding over extensive flat areas associated to subaqueous ripples laminae	PT-2 (subaqueous ripple laminae)

Table 1. Brief description of sedimentary units identified for the Avilé Member in Pampa de Tril San Eduardo localities. Modified from Veiga *et al.* (2002).

2006). Wind ripples typically develop as the result of saltation and creep transport (Mountney, 2006); when sediment accumulation occurs, these ripples climb, stack, or step over each other (Allen, 1968), producing a variety of laminae types that Hunter (1977) referred to as climbing-ripple structures. The presence of these types of laminae, resulting of grainfall, grainflow and wind-ripple deposition processes associated with large planar to tangential cross-bedded sandstones, suggests accumulation associated to the migration of slip-faced aeolian dunes (Collinson and Mountney, 2019).

Aeolian sand sheet

Description. Tabular bodies whose thickness ranges from 1 to 2 m, and width reaches hundreds of metres. Their lower boundaries are sharp, horizontal, and truncate aeolian dune units, while the upper boundaries are also sharp and horizontal, and are typically overlain by aeolian dune deposits or distal flood deposits. These bodies consist of fine- to medium-grained sandstones, well to moderately sorted, arranged in thin, relatively horizontal, inversely graded laminae with bimodal grain-size distributions. Discontinuous, centimetre-scale cross-laminated sets and preserved ripples with high ripple index are also present.

Interpretation. Horizontally laminated sandstones with bimodal grain size and preserved ripples are interpreted as wind-ripple lamination of the subcritically climbing translatent type (Hunter, 1977), as previously described for the aeolian dune unit. The presence of tabular bodies with only horizontal internal lamination and the absence of inclined bedding suggests that these are wind-laid deposits that were not able to construct aeolian dune bedforms. Although these characteristics could correspond to both dry interdune and sand sheet deposits, their common position above sharp, horizontal surfaces, and the lack of intertonguing with adjacent dune units, indicate that their accumulation was not contemporaneous with dune formation and therefore these deposits correspond to aeolian accumulation in sand sheets (Veiga *et al.*, 2002; Mountney 2006).

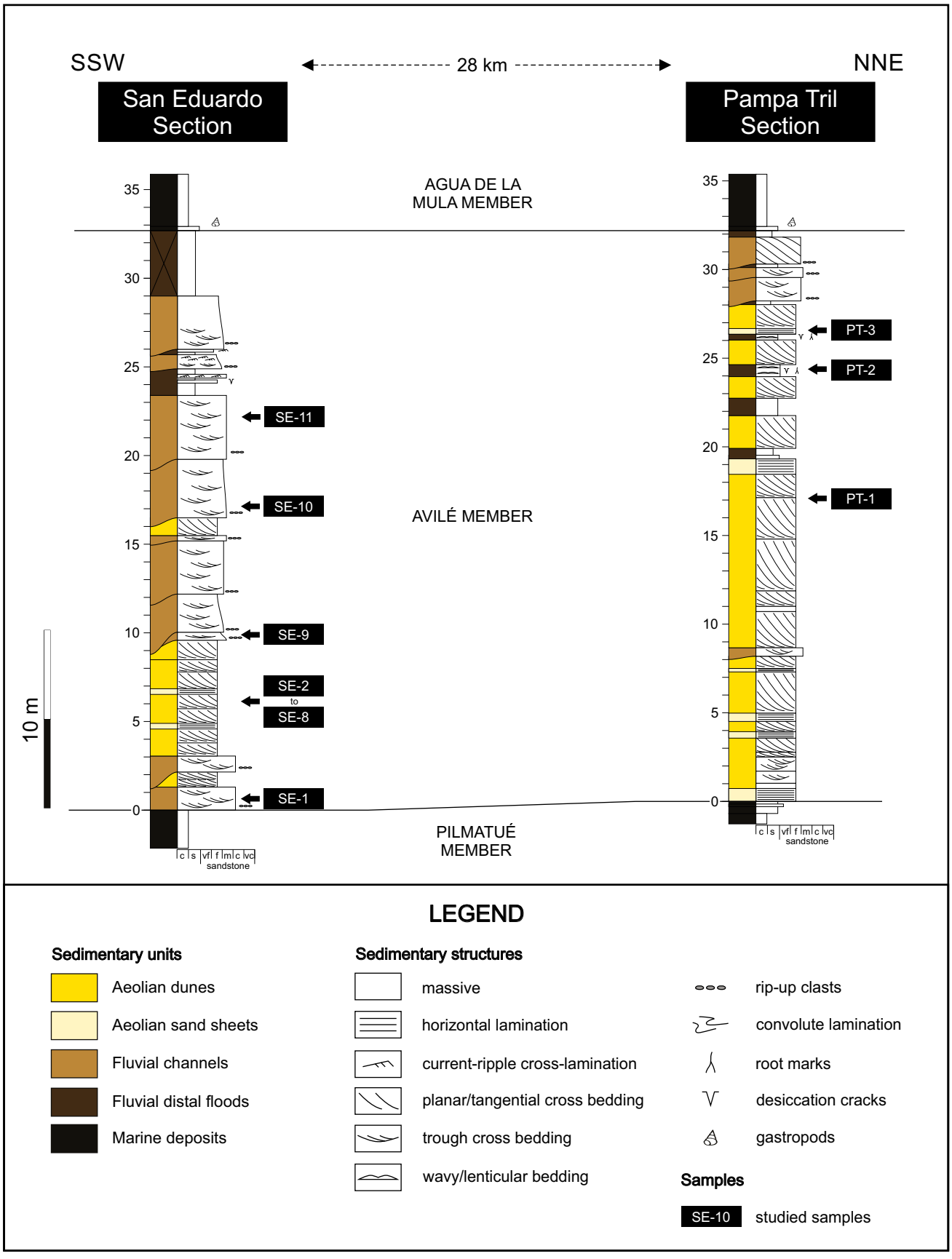

Figure 3. Sedimentary units present in San Eduardo and Pampa Tril sections, and location of the studied samples (modified from Prámparo and Veiga, 2024).

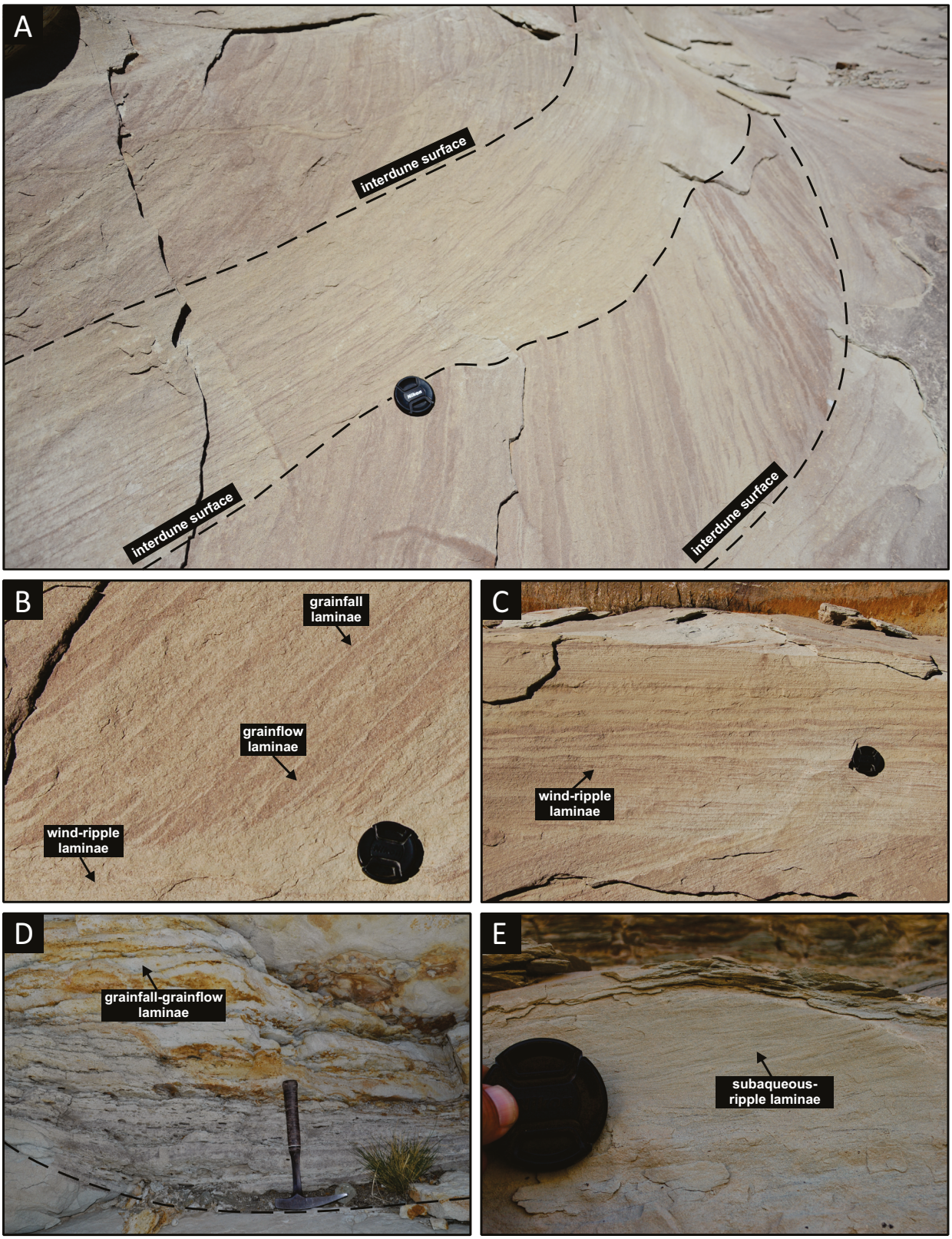

Figure 4. Field photos of the sandy sedimentary units identified by Veiga *et al.* (2002). **a)** Different Aeolian dune elements. In dashed lines, interdune surfaces are marked. **b)** Sandstones with tangential planar cross-bedding composed of grainflow, grainfall and wind-ripple laminae corresponding to the Aeolian dune elements. **c)** Sandstones arranged in tabular bodies with wind-ripple laminae corresponding to the Aeolian sand sheet elements. **d)** Sandstones arranged in lenticular bodies with trough cross-bedding and abundant rip-up clasts corresponding to the elements of Fluvial channels. In dashed lines is marked the base of the Fluvial channel element. e) Sandstones with subcritical climbing ripple-lamination corresponding to the elements of Distal fluvial floods. Lens cap: 7 cm. Hammer: 33 cm.

Fluvial channels

Description. These sedimentary units exhibit a lenticular cross-sectional geometry, with up to 5 m in thickness and tens of metres wide, vertically and laterally associated with fine-grained sandstones and mudstones. The lower boundaries are highly erosional, while the upper boundaries are either flat and sharp or gradually transitional into overlying fine-grained sandstones and mudstones. Most of these bodies are composed of medium-grained sandstones with well-developed trough cross-bedding and lack major internal erosion surfaces, corresponding to simple ribbons. The foresets are composed of thick, massive laminae, and no alternation between different types of laminae can be distinguished. Thin layers of rip-up clast conglomerates are commonly found at the base of the cross-bedded sets. Although most units display a simple internal fill, some sandstone bodies exhibit a more complex internal architecture, characterised by multiple major scouring surfaces that define distinct storeys (complex ribbons).

Interpretation. Both types of fluvial channel ribbons have thick, massive laminae in the trough cross-bedded sandstones that are interpreted to be the result of grainfall and/or grainflow processes on the lee slopes of three-dimensional dunes (Collinson and Mountney, 2019). Given the absence of diagnostic features to reliably differentiate between grainflow and grainfall deposits, no distinction was made. Considering the identification of internal features such as the primary mechanical sedimentary structure, the lenticular geometry of the sandstone bodies, and their vertical and lateral association with fine-grained floodplain deposits, these units are interpreted as the result of deposition associated to migration of subaqueous three-dimensional dune bedforms, formed as a consequence of channelised unidirectional currents (Veiga *et al.*, 2002; Bridge, 2003; Veiga *et al.*, 2007). In terms of architectural complexity, for the first type of channel units the predominance of simple channels with stable margins suggests the development of single low-sinuosity fluvial channels (Veiga *et al.*, 2002). Alternatively, the less abundant lenticular bodies that exhibit multiple, subparallel concave accretion surfaces are interpreted as the result of high-sinuosity fluvial channels (Veiga *et al.*, 2002).

Distal fluvial floods

Description. These sedimentary units are laterally extensive tabular to wedge-shaped bodies, up to 4 m thick and hundreds of metres wide, with sharp and horizontal upper and lower boundaries. These are intercalated between aeolian dune and sand sheet units (Fig. 3). These bodies are composed mainly of mudstones, siltstones and very fine-grained sandstones. Internally, they exhibit 2 to 15 cm thick massive to laminated claystones and siltstones with abundant root traces and sand-filled desiccation cracks. In addition, 5 to 20 cm thick couplets of laminated mudstones interbedded with massive or asymmetrical cross-laminated, very fine-grained sandstones are present.

Interpretation. The deposition of mudstones in these deposits is interpreted as the consequence of settling from suspension (Collinson y Mountey, 2019) and the massive or asymmetrical cross-laminated, very-fine grained sandstones, closely associated with laminated mudstones, are interpreted as tractional episodes related to the migration of subcritical subaqueous ripples (Allen, 1962). The presence of laterally extensive laminated mudstones alternating with sandstone–mudstone couplets suggests the combination of ponded water accumulation and repeated flooding over these extensive flat areas (Coronel *et al.*, 2020). These flooding processes associated with a relatively high water table led to the accumulation of these muddy units under subaqueous conditions with occasional, sand-grained sheetfloods reaching the distal areas (Coronel *et al.*, 2020). Moreover, sand-filled desiccation cracks within fine-grained deposits also indicate that standing-water accumulations were only temporary (Collinson and Mountney, 2019).

MICROSCOPIC ANALYSIS

The integrated analysis of petrographic grain size and fabric data from the five identified lamina types led to the characterisation of five distinct microfacies: three (Microfacies 1 to 3) associated with aeolian dune and sand sheet deposits (Figs. 5, 6 and 7) and two (Microfacies 4 and 5) with fluvial channels and flood deposits (Figs. 8 and 9).

Microfacies 1 is defined based on the characterisation of aeolian grainflow laminae,

which, together with interbedded aeolian grainfall laminae (Microfacies 2), constitute some of the cross-stratified sets of aeolian dune units (Figs. 5 and 6). Microfacies 3 is derived from the study of wind-ripple laminae (mainly subcritically climbing translatent strata), which occurs in aeolian dune and aeolian sand sheets units (Fig. 7). Microfacies 4 results from the analysis of subaqueous grainflow/grainfall laminae forming cross-stratified sets within fluvial channel (Fig. 8), while Microfacies 5 originates from the analysis of sandy laminae that, in regular alternation with muddy laminae, show subaqueous, subcritically climbing, ripple lamination in distal flood deposits (Fig. 9).

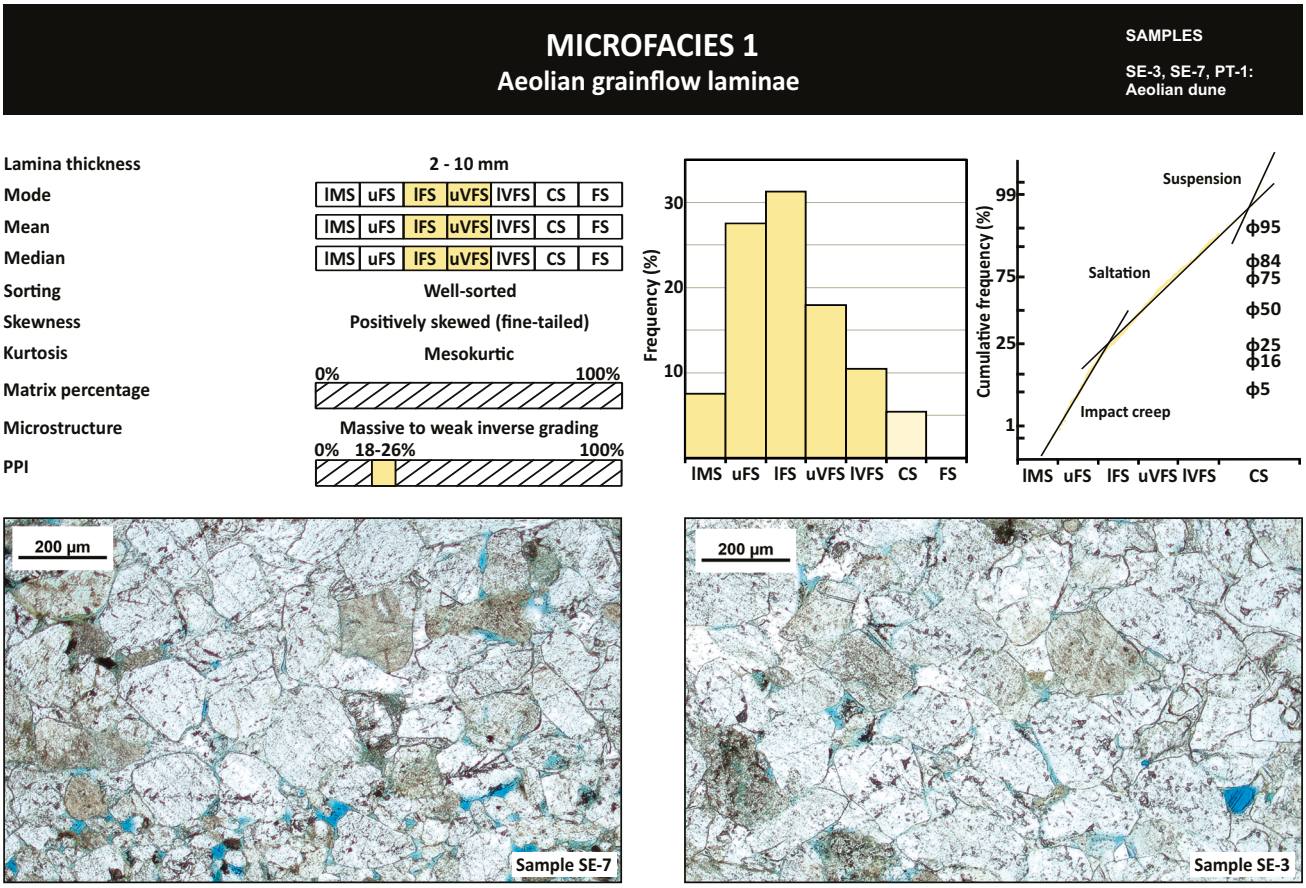

Figure 5. Grain size and fabric characteristics of Microfacies 1.

Microfacies 1 (MF1): aeolian grainflow laminae

Microfacies 1 characterises aeolian grainflow laminae which, intercalated with aeolian grainfall laminae (MF2), constitute cross-stratified sets of aeolian dune units (Fig. 5). The recorded thicknesses for these laminae range from 2 to 10 mm. In terms of fabric heterogeneity, the laminae are massive or exhibit weak inverse grading. This grading ranges from coarse silt (CS) and lower very fine sand (lVFS) to upper fine sand (uFS) and, less frequently, lower medium sand (lMS). Packing proximity index ranges between 18 and 26%. The grain size distribution is characterised by modal, mean, and median values within the lower fine sand (lFS) and upper very fine sand (uVFS) intervals, showing a fine-tailed, mesokurtic, and well-sorted distribution. The dissection of the cumulative frequency curve reveals two truncations, located at 2.5-3 and 4.5 ϕ, which define three grain size subpopulations. The coarsest subpopulation (2 to 2.5–3 ϕ) was likely transported by impact creep, the intermediate fraction (2.5–3 to 4.5 ϕ) by saltation, and the finest fraction (4.5 to 5 ϕ), scarcely represented, by suspension —prior to the aforementioned destabilisation (Visher, 1969). Point contacts predominate and carbonate cement is present, primarily in the interstitial space of coarser grains.

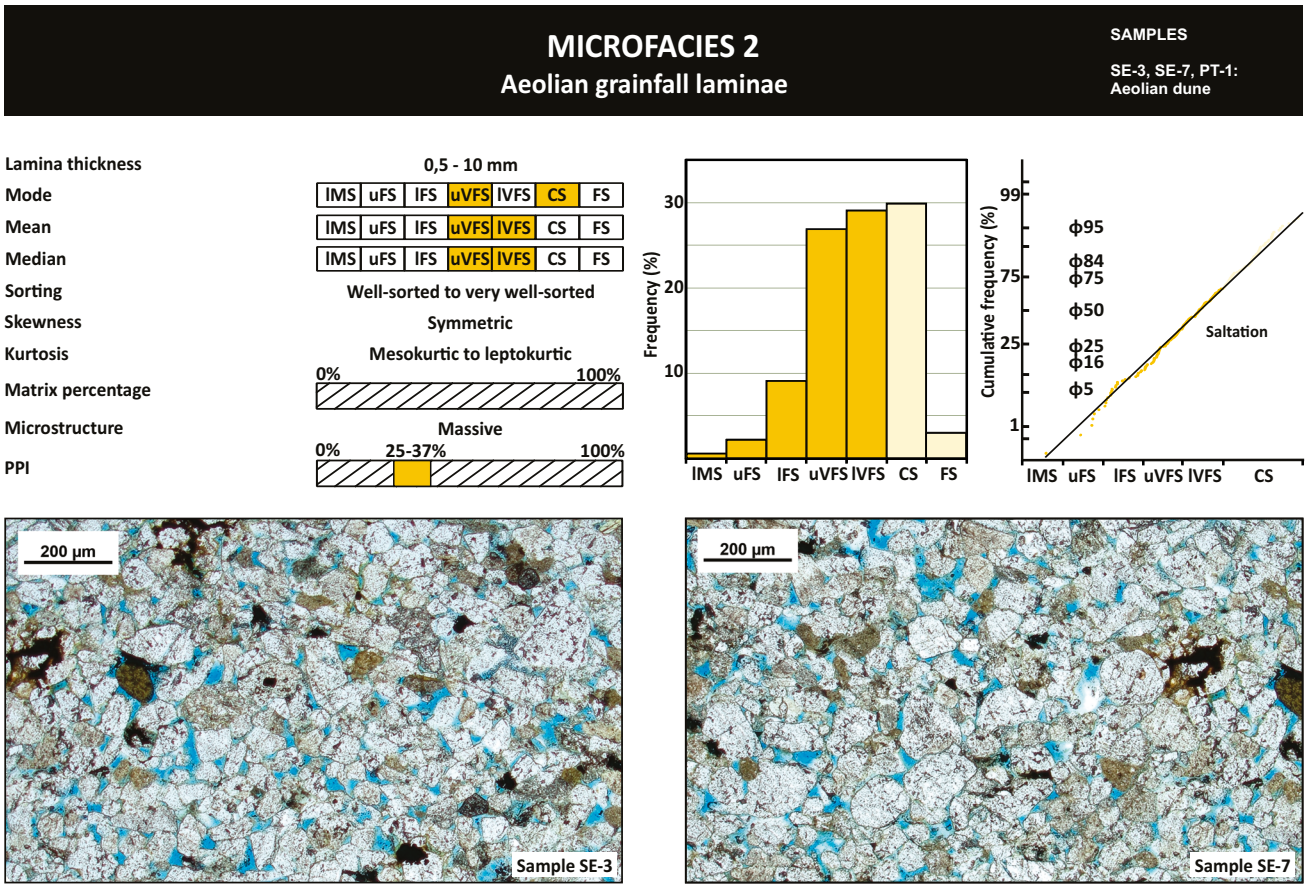

Figure 6. Grain size and fabric characteristics of Microfacies 2.

Microfacies 2 (MF2): aeolian grainfall laminae

Microfacies 2 characterises aeolian grainfall laminae, which, along with aeolian grainflow laminae (MF1), constitute cross-stratified sets within aeolian dune units (Fig 6). The thicknesses calculated for these laminae range from approximately 0.5 to 10 mm. Regarding the fabric heterogeneity, the laminae are classified as massive, reflecting minimal grain size segregation. The packing proximity index ranges from 25 to 37%. The grain size of this microfacies shows modal values corresponding to coarse silt (CS) and upper very fine sand (uVFS), with mean and median values in the lower very fine sand (lVFS) and upper very fine sand (uVFS) ranges. The grain size distribution is symmetric, mesokurtic to leptokurtic, and well to very well sorted, and the cumulative frequency curve lacks significant truncations. This latter aspect suggests that the entire grain-size population was mainly transported by saltation before crossing the dune crest and settling on the lee slope. The identified contact types in these laminae are predominantly point contacts, and the cement is relatively scarce, consisting mainly of ferruginous and carbonate materials.

Microfacies 3 (MF3): wind-ripple laminae

Microfacies 3 characterises wind-ripple laminae, which are present both in aeolian dune and aeolian sand sheets unit (Fig. 7). The recorded thicknesses for these laminae range from 1 to 8 mm. Regarding fabric heterogeneity, inverse micrograding is typically identified. Occasional alignment of the apparent major axis of components parallel to the lamination is also noted. The packing proximity index varies depending on the part of the lamina being analysed, with values ranging from 26 to 40%. In the upper portion of the laminae, where the grain size tends to be coarser, the packing is looser than in the basal areas. The grain size distribution of this microfacies includes modal, mean, and median values within the lower very fine sand (lVFS) and upper very fine sand (uVFS) intervals. The distribution is symmetric to slightly negatively skewed (coarse-tailed), mesokurtic to leptokurtic, and well-sorted.

The cumulative frequency curve, without significant truncations, likely reflects transport dominated by saltation. Point contacts predominate, and the identified cement is mainly carbonate.

Microfacies 4 (MF4): subaqueous grainflow/ grainfall laminae

Microfacies 4 results from the analysis of laminae forming cross-stratified sets within fluvial channel units (Fig. 8). The thickness of the laminae in this microfacies could not be precisely determined, as it exceeds the dimensions of the thin sections analysed (greater than 30 mm). The microstructure is classified as massive, with no evident preferential orientation of clastic components. Occasionally thin, diffuse laminae just a few millimetres thick, composed of relatively finer material, are observed. The packing proximity index is highly variable, ranging from 25 to 50%. The grain size is characterised by modal values within the lower fine sand and upper very fine sand (lFS-uVFS) intervals, with mean and median values corresponding to upper very fine sand (uVFS). The distribution is symmetric, mesokurtic, and well-sorted, and the dissection of the cumulative frequency curve identifies a single truncation at 4.5 ϕ, which divides the grain size population into two transport subpopulations: saltation and suspension. Both point and concavo-convex contacts are present, with carbonate, siliceous and argillic cement.

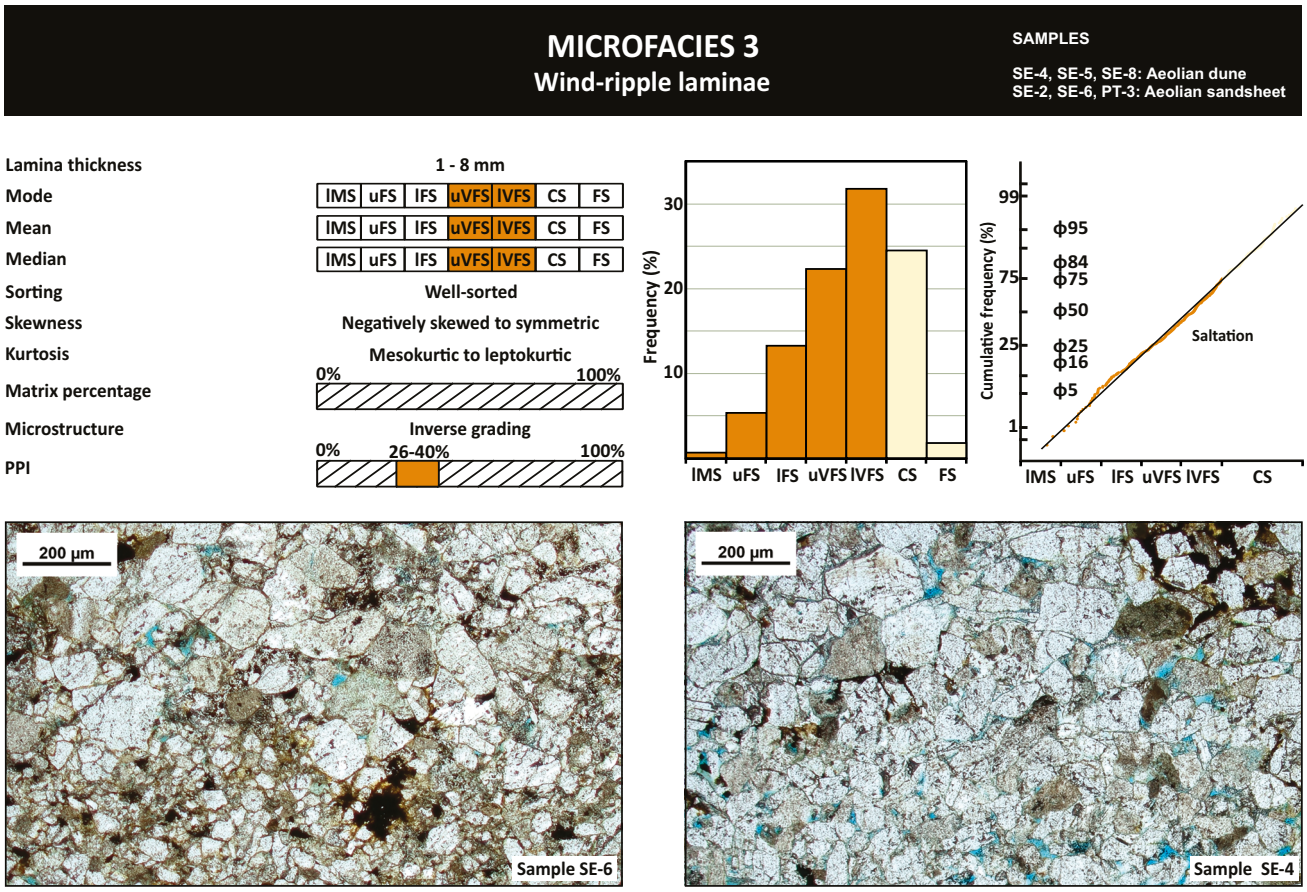

Figure 7. Grain size and fabric characteristics of Microfacies 3.

Microfacies 5 (MF5): subaqueous-ripple laminae

Microfacies 5 characterises sandy laminae that, in regular alternation with muddy laminae, constitute subaqueous ripple lamination present in the deposits of distal flood units (Fig. 9). The thickness of the cross-lamination sets exceeds 30 mm, while individual sandy laminae, bounded by thin and discontinuous layers of muddy material, vary between 0.5 and 1.5 mm in thickness. No

fabric patterns are observable at the microscopic scale, so the microstructure is classified as massive. The Packing proximity index ranges between 20% and 34%.

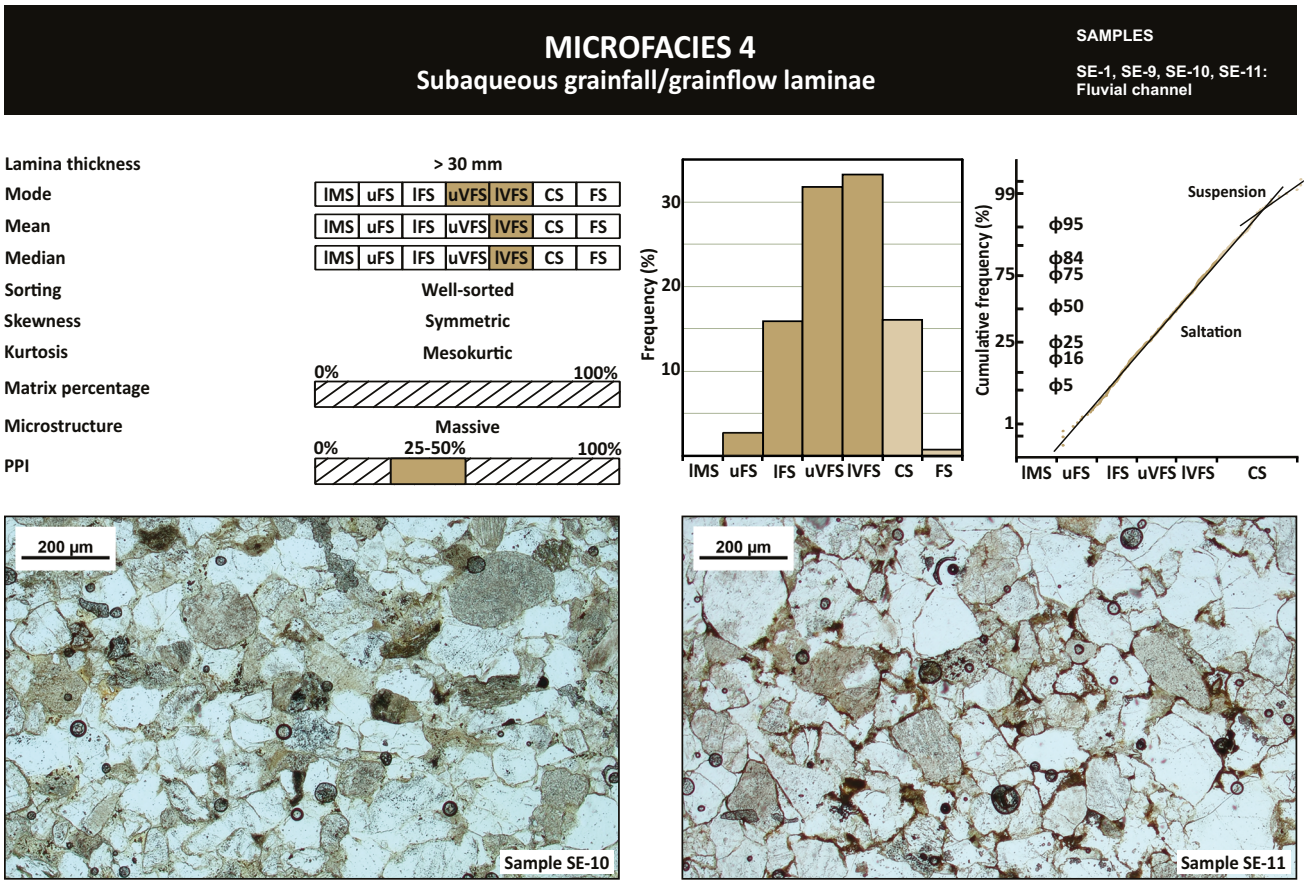

Figure 8. Grain size and fabric characteristics of Microfacies 4.

Due to methodological limitations in analysing clay-sized grains, the textural analysis was applied only to the sandy and silty fractions of the laminae. This microfacies has a grain size range that allows for the discrimination between a pelitic matrix, comprising approximately 24%, and a grain framework with modal, mean, and median values corresponding to lower very fine sand (lVFS). The distribution is positively skewed (fine tail), leptokurtic, and well-sorted. A single truncation was identified near 4 ϕ in the cumulative frequency curve, indicating two transport subpopulations prior to grainflow/grainfall deposition: saltation and suspension. No cement was observed in this microfacies.

MICROFACIES VARIABILITY

Aeolian microfacies

In general terms, good sorting and the absence of matrix are features present in all aeolian microfacies (MF 1 to 3). At the same time, it is noted that these differ, to a greater or lesser extent, in grain-size central-tendency and skewness parameters, as well as in their microstructure and packing (Fig. 10).

MF1 (aeolian grainflow laminae) shows the highest modal, mean, and median values, with a grain-size range extending from upper very fine sand (uVFS) to lower fine sand (lFS). In contrast, MF2 (aeolian grainfall laminae) shows the lowest values, within a range between coarse silt (CS) and upper very fine sand (uVFS). This is because the processes forming the different types of stratification within aeolian dunes sort the incoming grain population into distinct subpopulations. Saltation and reptation on the stoss slope generate two grain-size subpopulations with different behaviours upon reaching the brink. Finer grains, transported primarily by saltation, tend to fall down the lee side due to deceleration and flow separation. Coarser grains, transported by reptation, accumulate at the

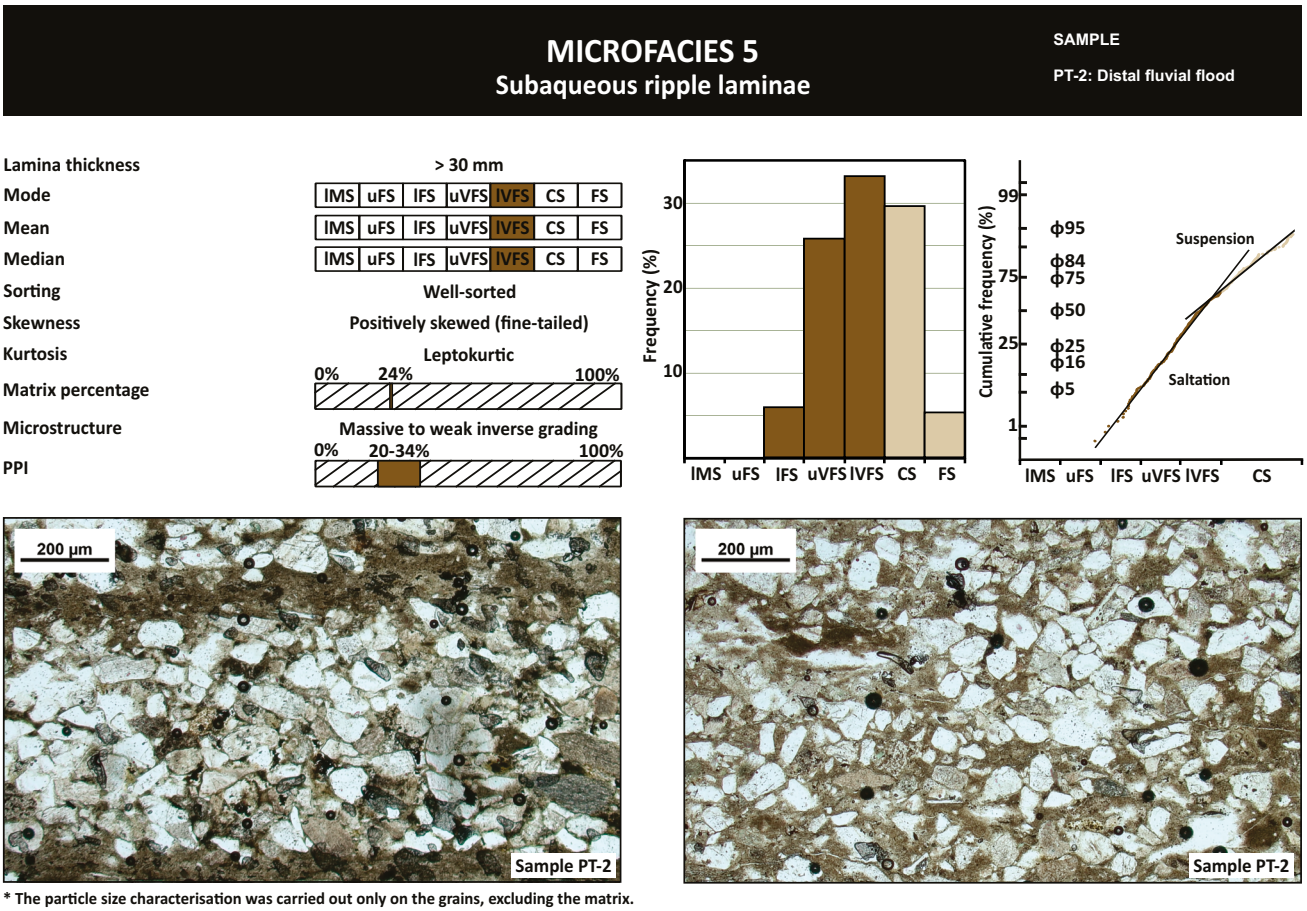

Figure 9. Grain size and fabric characteristics of Microfacies 5. The particle size characterization was carried out only on the grains, excluding the matrix.

crest and are periodically destabilised, triggering grain avalanches (Kocurek and Dott, 1981). Notably, finer grains initially deposited by grainfall are often later incorporated into grainflows, which explains the similarity between MF2 textures and the basal portion of MF1 laminae.

Laminae generated by grainflow (MF1) are thicker than other types of laminae present in aeolian dunes. Hunter (1977) found that this type of laminae can reach thicknesses of 20-50 mm and is often even thicker when the grainflow reaches the base of the dune. However, Clemmensen and Abrahamsen (1983) observed grainflow laminae just a few millimetres thick and interpreted some of the thicker laminae as multistorey layers, formed by successive grainflow events. Conversely, Fryberger and Schenk (1981) indicated that the thickness of grainfall deposits (MF2) is highly variable, influenced by the deposition rate and the duration of wind events. Limarino *et al.* (2015) documented intervals several tens of centimetres thick, attributed to stacked grainfall laminae deposited without intercalated grainflow or ripple migration events. Regarding the wind-ripple laminae (MF3), their thickness is influenced by deposition and ripple migration rates, as well as by ripple morphology (Fryberger and Schenk, 1981).

Microstructural differences are evident among the three aeolian microfacies. While both MF1 (grainflow laminae) and MF3 (wind-ripple laminae) commonly exhibit inverse grading, the pattern in MF1 is typically weak and abrupt. This contrast likely results from the distinct depositional mechanisms behind each microstructure (Schenk, 1983). The eventual weak inverse grading present in MF1 is due to the phenomenon known as shear sorting, which consists of the settling of finer grains and the ascent of coarser grains due to coexisting interstitial settling and dispersive pressure within a sediment mass subjected to shear (Bagnold, 1941). On the other hand, the well-developed inverse grading of MF3 is related to the fact that during the migration of aeolian

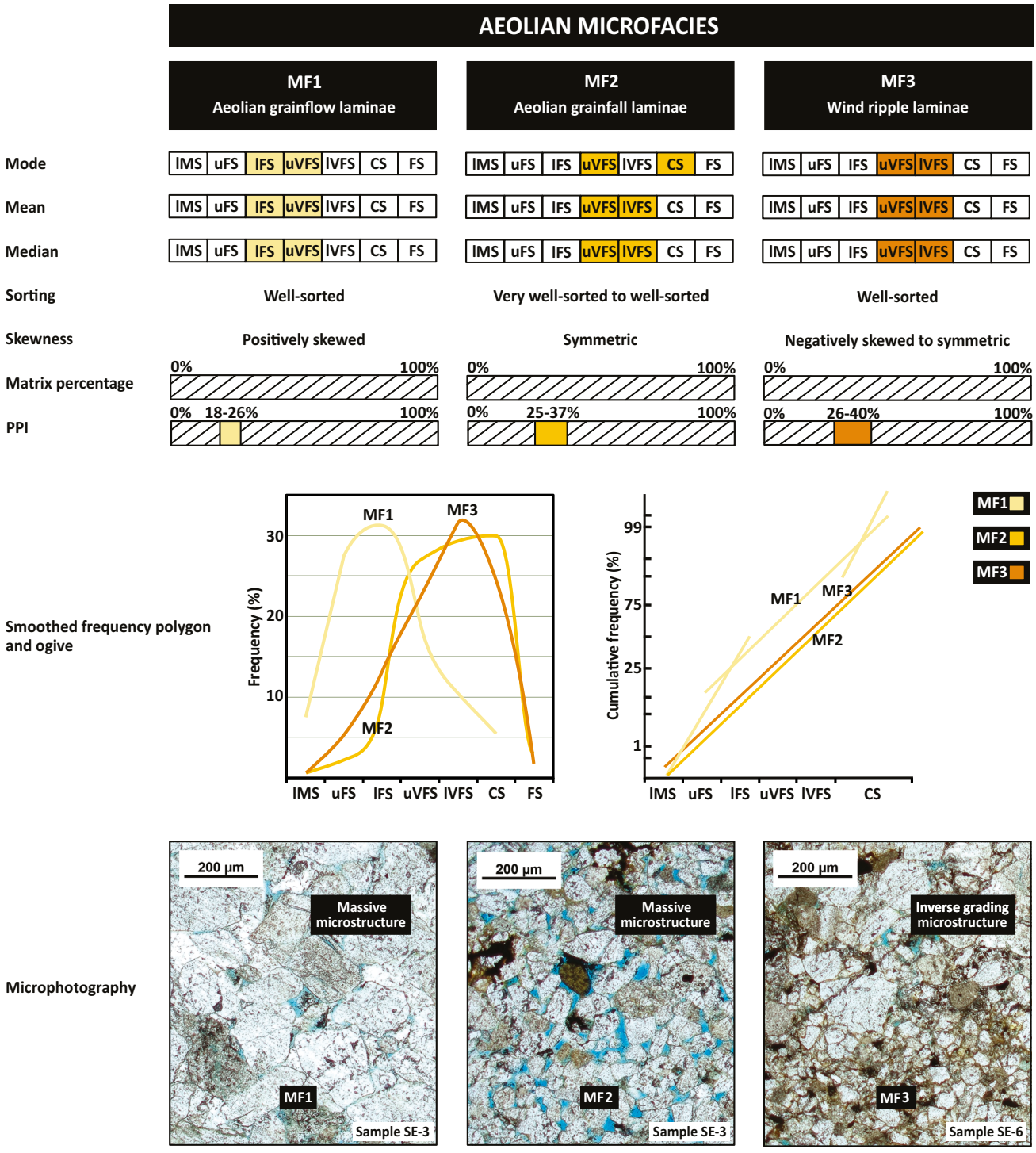

Figure 10. Comparative analysis of aeolian microfacies.

ripples, the coarser subpopulation, mobilised by reptation, tends to accumulate on the crests and lee slopes of the ripples, covering in the migration process the finer subpopulation transported by saltation and that tends to concentrate in the troughs (Schenk, 1983). The inverse grading is the most characteristic feature of this type of lamina, as no other aeolian depositional process produces this attribute so repeatedly (Schenk, 1983). In contrast, MF2 typically presents a massive structure, consistent with the low degree of grain-size segregation involved in grainfall processes (Hunter, 1977). However, Schenk (1983) pointed out that its texture can vary depending on wind velocity history.

Packing proximity index (PPI) values also allow distinguishing between the three aeolian microfacies. MF1 shows the loosest packing (PPI between 18–26%), explained by the rapid deceleration of sand flows during grain avalanching (Allen, 1982). In contrast, MF3 displays the tightest packing (PPI between 26–40%), a consequence of tractive deposition during ripple migration (Schenk, 1983; Limarino *et al.*, 2015). MF2 shows intermediate packing values (PPI between 25–37%), slightly lower than MF3 but higher than MF1. These relative values are consistent with observations by Schenk (1983), who asserted that grainfall deposits exhibit variable primary porosity but are generally intermediate between layers formed by grain avalanches and by ripple migration.

Fluvial microfacies

No significant similarities were observed between the two fluvial microfacies described, except for the good sorting and the massive microstructure present in both cases. Significant differences related to grain-size central-tendency measures, matrix content, and packing were identified (Fig. 11).

MF4 (subaqueous grainfall/grainflow laminae) shows modal, mean, and median values ranging from lower very fine sand (lVFS) to upper very fine sand (uVFS). These values are higher than those observed in MF5 (subaqueous-ripple laminae), whose grain size parameters fall within the lower very fine sand (lVFS) range—even when the matrix was excluded from the analysis. This textural difference may be attributed both to the lower selective capacity of the sedimentary process involved in MF5 and to the relative positions of the sedimentary units within the fluvial system. MF4 is related to fluvial channel units, located in more proximal sectors of the sedimentary environment, where proximity to the source area and the discharge and slope conditions favour the deposition of coarser material and limit the settling of finer particles. In contrast, MF5 corresponds to the distal fluvial flood units, where fine sediments are abundant, and the accumulation of mudstones in periodically interrupted with tractional episodes associated to migration of subcritical subaqueous ripples.

According to Visher (1969), the presence of a single truncation near 4 ϕ in both microfacies indicates the involvement of two transport mechanisms: saltation and suspension. In the case of MF4, it is important to clarify that this refers to the transport processes operating prior to the development of grainflows. In both cases, the microstructure is massive, reflecting the incapacity of the transporting fluid to generate an internal grain arrangement within individual laminae. Moreover, MF4 exhibits tighter packing (PPI between 25 and 50%) compared to MF5 (PPI between 20 and 34%), although in both microfacies, abundant grain–matrix contacts are observed.

Comparison of fluvial and aeolian microfacies

To analyse microfacies characteristic related to analogous depositional mechanisms but related to different transport and depositional agents, comparisons were made between MF1/MF2 and MF4, linked to the migration of aeolian dunes and fluvial dunes respectively (Fig. 12), as well as between MF3, associated with the migration of wind ripples, and MF5, generated by the migration of subaqueous ripples (Fig. 13).

MF1, MF2 and MF4 (all three associated with dune migration) share good sorting and lack of matrix. MF4 exhibits measures of central tendency that are intermediate between MF1 and MF2, with asymmetry resembling the symmetrical distribution of MF2, and a massive microstructure that characterises both MF2 and, eventually, MF1. These similarities may partly arise from the fact that almost all subaqueous grainfall deposits are typically incorporated into subsequent subaqueous grainflows (Hunter and Kocurek, 1986). This is further linked to the observation that subaqueous grainflow laminae are almost invariably in contact with each other, unlike aeolian grainflow laminae, which are commonly separated by grainfall deposits (Hunter, 1985). For these reasons, distinguishing between laminae formed by continuous subaqueous grainflow and those formed by subaqueous grainfall is highly complex (Hunter and Kocurek, 1986). The thickness of the laminae in MF4 (greater than 30 mm), which are significantly greater than those in MF1 (2-10 mm) and MF2 (1-8 mm), further support this interpretation. A notable difference is also seen in the higher PPI values for MF4 (25 and 50%) compared to MF1 (18–26%) and MF2 (25–37%).

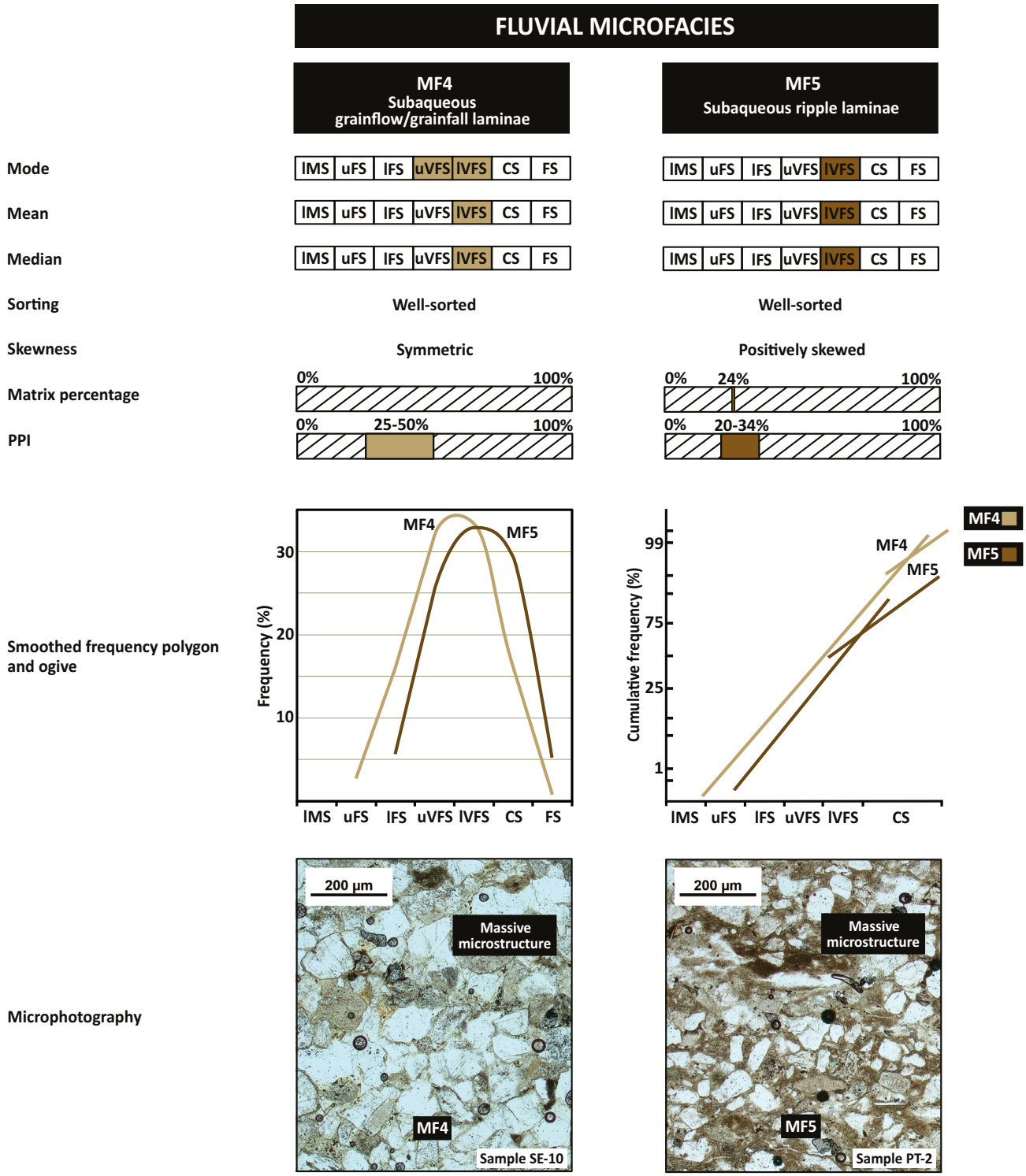

Figure 11. Comparative analysis of fluvial microfacies.

For MF3 and MF5 (both related to ripple migration) the only resemblance is in terms of sorting and packing, although the latter presents slightly lower PPI values, possibly due to the presence of fine interstitial material (matrix). Unlike MF3, where each lamina represents the depositional product of the climbing of an individual wind ripple, in MF5 each lamina is part of the cross-lamination foreset. This occurs because the foresets of the wind-ripple lamination are not visible, as the studied laminae correspond to translatent strata (Hunter, 1977). The difficulty of identifying

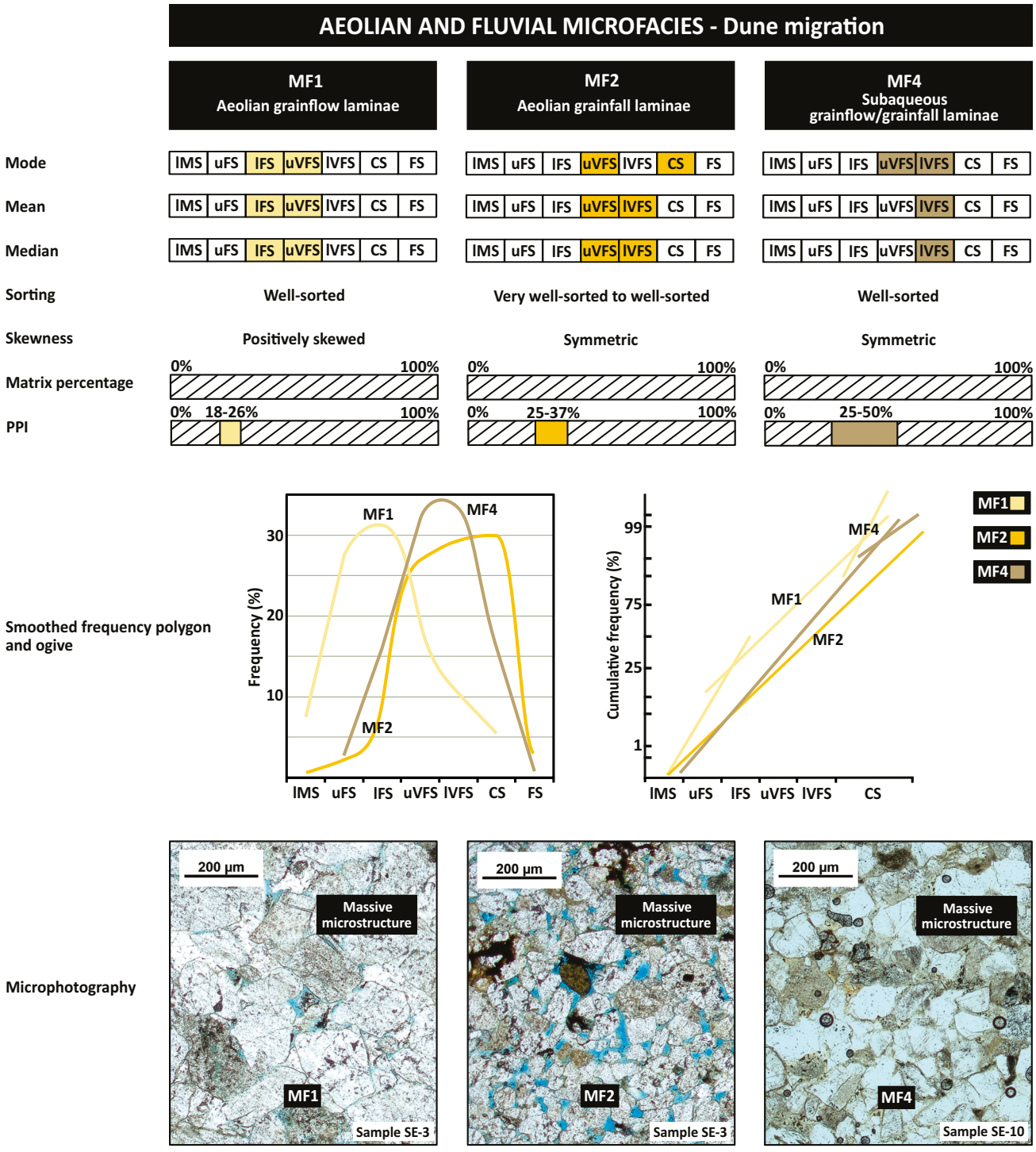

Figure 12. Comparative analysis of aeolian and fluvial microfacies linked to the migration of aeolian and subaqueous dunes.

boundaries between foresets in MF3 may be linked to insufficient fluctuations in the grain size of the sand reaching the leeward side of the wind ripples (Hunter, 1977) and to the fact that the sand reaching this sector does not experience avalanche mechanisms (Schenk, 1983). In contrast, Kocurek and Dott (1981) argue that the cross-lamination generated by the migration of subaqueous ripples is clearly distinguishable, as each foreset results from "mini-avalanching" mechanisms. In the studied laminae, this distinction is further enhanced by the alternation with muddy laminae. The massive microstructure observed in MF5 laminae may be related to the fact that, in subaqueous ripples, the

coarser material does not accumulate in the crest area —a key factor in the inverse grading generated during wind ripple migration (MF3).

MICROFACIES APPLICABILITY

Research on upscaling reservoir properties (*i.e.*, the process of translating small-scale petrophysical data into parameters usable at reservoir scale) highlights the importance of incorporating small-scale heterogeneities to generate more realistic and predictive, analogue-based, field-scale reservoir models (Pickup *et al.*, 1994; Pringle *et al.*, 2006; Henares *et al.*, 2016). When studying heterogeneous reservoirs such as those derived from fluvial and aeolian interactions in space and time, particular care is required, especially at the microscale, where diverse laminae types can be present and affect capillary forces, influencing both the initial hydrocarbon distribution and subsequent water injection/flood oil recovery (Ringrose and Bentley, 2021). Huang *et al.* (1995) demonstrated that the presence of low permeability laminae can induce localised capillary trapping due to elevated water saturations during the displacement of oil by water. Furthermore, the effect of fine-scale heterogeneity on fluid flow is strongly modulated by wettability conditions (Huang *et al.*, 1996). Within a single reservoir, wettability may vary spatially, with lower permeability laminae tending to be more oil-wet and higher permeability intervals more water-wet. This contrast enhances the potential of capillary trapping, especially in predominantly water-wet systems, where such trapping mechanisms become more pronounced and require more careful consideration in reservoir performance assessments. Therefore, the analysis of textural heterogeneity at the microscopic scale approached through the study of microfacies is extremely important. This strategy enables a precise interpretation of the heterogeneity present within sedimentary units, since these layers represent the basic structural building blocks from which all larger structures are made (Hunter, 1977; Limarino *et al.*, 2015).

The textural characteristics defining microfacies, closely linked to their depositional origins as described above, are linked to petrophysical parameters such as porosity and permeability, which are relevant for identifying intervals of interest during the evaluation of hydrocarbon reservoir rocks at advanced stages of development (Limarino *et al.*, 2025). For instance, the slightly coarser grain size and looser packing of the aeolian grainflow laminae (MF1), when compared with the other aeolian lamina types, may be reflected in significantly higher permeability values. In fact, aeolian grainflow laminae have been reported to show permeability values up to an order of magnitude greater than those formed by aeolian grainfall or wind ripple migration (Howell and Mountney, 2001). Considering the relationship between microfacies and petrophysical properties, and acknowledging that the spatial distribution of microfacies is not random but occurs in systematic associations related to the different sedimentary units, their detailed analysis becomes essential for accurate reservoir characterisation and predictive modelling. This approach then represents a very interesting complement, although architectural studies derived from fieldwork are essential, given the importance of considering fundamental characteristics such as the geometry and dimensions of the rock bodies.

A more robust definition of the diagnostic characteristics of each microfacies, supported by the mesoscale information provided by fieldwork, would provide a high degree of reliability for assigning a specific origin to the deposits in core studies. For example, distinguishing whether a cross-stratified set corresponds to MF1–MF2 or to MF4 could allow to differentiate between aeolian dune and fluvial channel deposits. This distinction could be important in reservoir modelling, as it can help guide decisions regarding geometry and dimensions of the sedimentary bodies. Specifically in the Avilé Member, aeolian dune deposits form laterally continuous tabular bodies, whereas fluvial channels tend to be expressed by lenticular units with limited lateral continuity (Veiga *et al.*, 2002; Rossi and Masarik, 2002). Laminae showing MF1 not only exhibit textural features associated with favourable petrophysical properties, but also constitute extensive, tabular bodies. In contrast, laminae related to MF4, despite having similar textural characteristics, is spatially restricted to lenticular bodies with limited lateral extension. Therefore, as Limarino *et al.* (2015) stated, the study of microfacies can be considered a valuable tool when analysing subsurface samples.

Another interesting aspect is that the relative abundance of the various identified microfacies

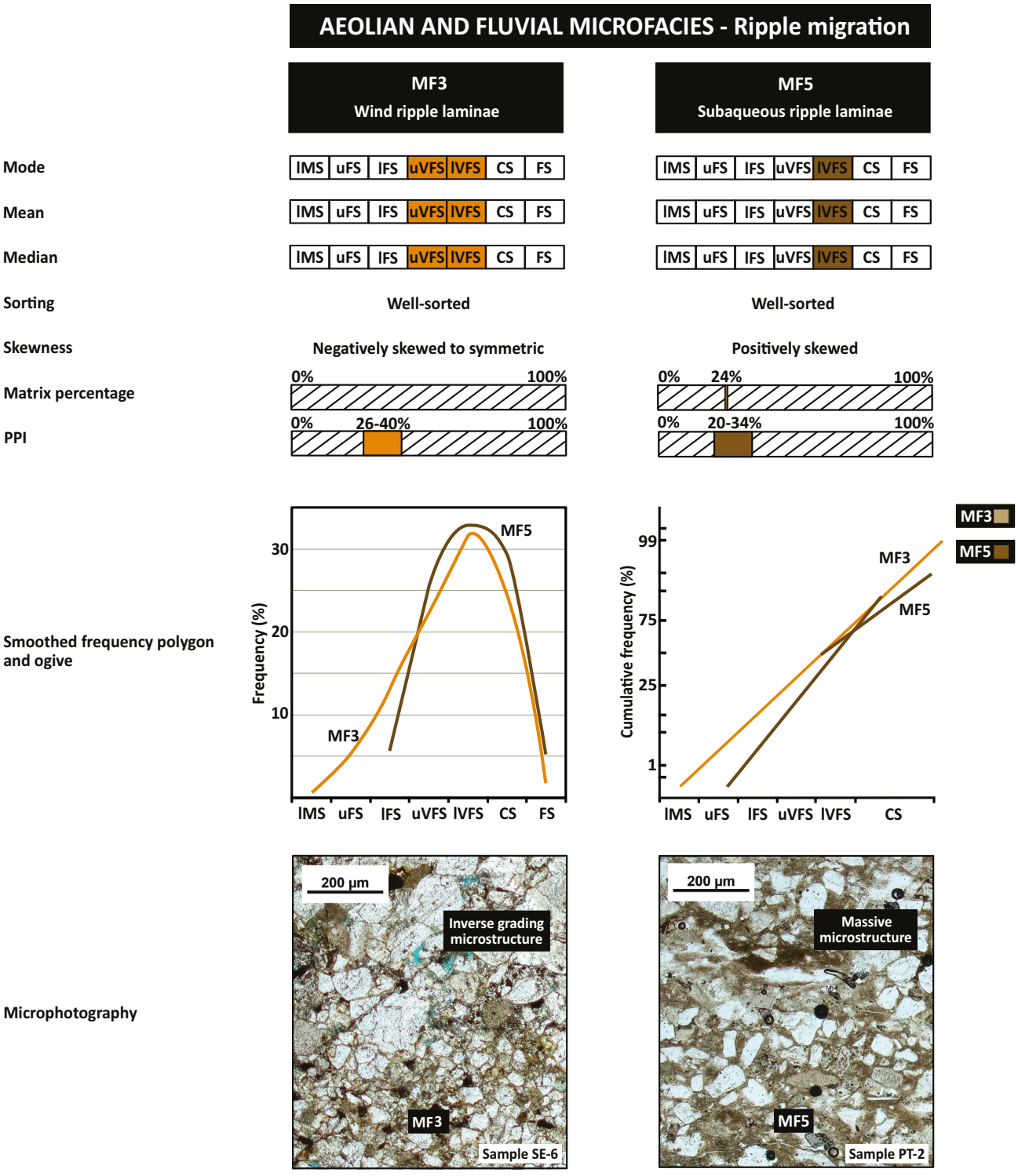

Figure 13. Comparative analysis of aeolian and fluvial microfacies linked to the migration of wind and subaqueous ripples.

could be considered to represent the relative dominance of certain depositional mechanisms during the formation of the studied deposits. It could provide detailed information regarding the dynamics and morphology of the medium-scale bedforms involved in the rock record, allowing for a refinement of the assigned depositional models. For example, aeolian dunes dominated by MF1 and those dominated by MF3 are expected to differ not only in the textural characteristics of the resulting deposits,

but also in their morphology and dynamics, given the distinct depositional mechanisms involved.

It should be also considered that textural heterogeneity in sandstone reservoirs is influenced not only by variations in depositional facies, but also by diagenetic processes (De Ros, 1998). In particular, small-scale porosity and permeability changes has a strong impact on the distribution and magnitude of early diagenetic processes (Henares *et al.*, 2016). Understanding how deposition-induced and early diagenetic-induced heterogeneities are related is key to accurately predicting reservoir quality, since the evolution of the pore system is largely shaped by these early characteristics (Henares *et al.*, 2014). A more comprehensive understanding of how predictable depositional features interact with diagenetically induced heterogeneity could lead to more realistic reservoir models and improve strategies for oil recovery and bypassed oil exploitation (Limarino *et al.*, 2015).

CONCLUSIONS

Multiscale analysis of fluvial and aeolian sandstone laminae from the Avilé Member of Agrio Formation was conducted. The definition of four sandy-sedimentary units at a mesoscale, followed by the study of five microfacies, enabled the identification of significant differences as well as notable similarities in their corresponding textural parameters. Results demonstrate a strong link between microtextural characteristics and the sedimentary processes responsible for deposition. Importantly, it is shown that there are both differences among deposits formed by the same transport and depositional agent —*e.g.*, subaqueous grainflow/grainfall laminae (MF4) and subaqueous-ripple laminae (MF5)—, and similarities between aeolian and fluvial deposits formed by analogous depositional mechanisms —*e.g.*, aeolian grainflow (MF1) and grainfall (MF2) laminae and subaqueous grainflow/grainfall (MF4) laminae)—. Such findings suggest that the depositional process may exert greater control on deposit texture than the characteristics of the transport and depositional agent. The study contributes to a more accurate characterisation of small-scale heterogeneities, which is essential for improving facies modelling and reservoir prediction. Overall, the findings highlight the complexity of interpreting microtextural heterogeneity and underscore the value of detailed microfacies analysis as a complement to field studies for improved reservoir characterisation.

Acknowledgments. We would like to thank the Consejo Nacional de Investigaciones Científicas y Técnicas (grant number PIP#1122015-0100809) and the Universidad Nacional de La Plata (grant number N1015) for partially funding this project. Part of this study is the result of the first author's bachelor's degree thesis at the Facultad de Ciencias Naturales y Museo from the Universidad Nacional de La Plata. We gratefully acknowledge the substantial improvements contributed by the two anonymous reviewers.

REFERENCES

Aguirre-Urreta, M. B., and Rawson, P. F. (1997). The ammonite sequence in the Agrio Formation (Lower Cretaceous), Neuquén Basin, Argentina. *Geological Magazine, 134*(4), 449–458. https://doi.org/10.1017/S0016756897007206

Aguirre-Urreta, M. B., Rawson, P. F., Concheyro, G. A., Bown, P. R., and Ottone, E. G. (2005). Lower Cretaceous (Berriasian–Aptian) biostratigraphy of the Neuquén Basin. In G. D. Veiga, L. A. Spalletti, J. A. Howell, E. Schwarz (Eds.), *The Neuquén Basin, Argentina: A Case Study in Sequence Stratigraphy and Basin Dynamics*, Geological Society, London, Special Publications, 252, 57–81. https://doi.org/10.1144/GSL.SP.2005.252.01.04

Allen, J. R. L. (1962). Asymmetrical ripple marks and the origin of cross-stratification. *Nature, 194*(4824), 167–169. https://doi.org/10.1038/194167a0

Allen, J. R. L. (1968). The nature and origin of bed□form hierarchies. *Sedimentology, 10*(3), 161–182. https://doi.org/10.1111/j.1365-3091.1968.tb01110.x

Allen, J. R. L. (1982). *Sedimentary structures: Their character and physical basis* (Vol. 1). Elsevier.

Al-Masrahy, M. A., and Mountney, N. P. (2014). *Approaches to modelling stratigraphic heterogeneity in mixed fluvial and aeolian hydrocarbon reservoirs* [abstract]. 2014 AAPG Annual Convention and Exhibition, Houston, Texas. https://eprints.whiterose.ac.uk/id/eprint/83924/

Argüello, J. (2011). Yacimiento Puesto Hernández. In H. A. Leanza, C. Arregui, O. Carbone, D. N. Danieli, and J. C. Vallés (Eds.), *Geología y Recursos Naturales de la Provincia del Neuquén*, Relatorio del XVIII Congreso Geológico Argentino, 663–668. Asociación Geológica Argentina.

Argüello Scotti, A., Matías, M., Martino, L., Veiga, G. D., and Mayoral, J. P. (2022). Preserved eolian bedforms control reservoir heterogeneity: Characterization and modeling workflow for the Avilé Member, Neuquén Basin, Argentina. *Marine and Petroleum Geology, 146*, 105930. https://doi.org/10.1016/j.marpetgeo.2022.105930

Bentley, M., and Ringrose, P. (2021). *Reservoir Model Design: A Practitioner's Guide*. Springer.

Bagnold, R. A. (1941). *The physics of blown sand and desert dunes*. Methuen and Co. Ltd.

Bofill, L., Bozetti, G., Schäfer, G., Ghienne, J. F., Schuster, M., Heap, M. J., Knobelock, G., Scherer, C., Armenlenti, G. and de Souza, E. (2025). Sedimentary control on permeability heterogeneity: The middle Buntsandstein continental sandstones (Lower Triassic, eastern France). *Marine and Petroleum Geology, 173*, 107261. https://doi.org/10.1016/j.marpetgeo.2024.107261

Bokman, J. (1956). Terminology for stratification in sedimentary rocks. *Geological Society of America Bulletin, 67*(1), 125–126. https://doi.org/10.1130/0016-7606(1956)67[125:TFSISR]2.0.CO;2

Bridge, J. S. (2003). *Rivers and floodplains: forms, processes, and sedimentary record*. John Wiley and Sons.

Campbell, C. V. (1967). Lamina, laminaset, bed and bedset. *Sedimentology, 8*(1), 7–26. https://doi.org/10.1111/j.1365-3091.1967.tb01301.x

Clemmensen, L. B., and Abrahamsen, K. (1983). Aeolian stratification and facies association in desert sediments, Arran basin (Permian), Scotland. *Sedimentology, 30*(3), 311–339. https://doi.org/10.1111/j.1365-3091.1983.tb00676.x

Collinson, J., and Mountney, N. (2019). *Sedimentary structures*. Liverpool University Press.

Coronel, M. D., Isla, M. F., Veiga, G. D., Mountney, N. P., and Colombera, L. (2020). Anatomy and facies distribution of terminal lobes in ephemeral fluvial successions: Jurassic Tordillo Formation, Neuquén Basin, Argentina. *Sedimentology, 67*(5), 2596–2624. https://doi.org/10.1111/sed.12712

De Ros, L. F. (1998). Heterogeneous generation and evolution of diagenetic quartzarenites in the Silurian-Devonian Furnas Formation of the Paraná Basin, southern Brazil. *Sedimentary Geology, 116*(1–2), 99–128. https://doi.org/10.1016/S0037-0738(97)00081-X

Folk, R. L., and Ward, W. C. (1957). Brazos River bar [Texas]; a study in the significance of grain size parameters. *Journal of sedimentary research, 27*(1), 3–26. https://doi.org/10.1306/74D70646-2B21-11D7-8648000102C1865D

Friedman, G. M. (1958). Determination of sieve-size distribution from thin-section data for sedimentary petrological studies. *The Journal of Geology, 66*(4), 394–416. https://doi.org/10.1086/626525

Fryberger, S. G., and Schenk, C. (1981). Wind sedimentation tunnel experiments on the origins of aeolian strata. *Sedimentology, 28*(6), 805–821. https://doi.org/10.1111/j.1365-3091.1981.tb01944.x

Fryberger, S. G., Knight, R., Hern, C., Moscariello, A., and Kabel, S. (2011). Rotliegend facies, sedimentary provinces, and stratigraphy, Southern Permian Basin UK and the Netherlands: a review with new observations. In J. Grötsch and R. Gaupp (Eds.), *The Permian Rotliegend of the Netherlands*, SEPM Special Publication 98, 51–88. https://doi.org/10.2110/pec.11.98.0051

Gulisano, C., Minniti, S., Rossi, G., and Villar, H. J. (2001, November). *The Agrio petroleum system: Hydrocarbon contribution and key elements, Neuquén Basin, Argentina* [abstract]. 2001 AAPG Hedberg Research Conference: "New Technologies and New Play Concepts in Latin America", Mendoza.

Henares, S., Caracciolo, L., Cultrone, G., Fernández, J., and Viseras, C. (2014). The role of diagenesis and depositional facies on pore system evolution in a Triassic outcrop analogue (SE Spain). *Marine and Petroleum Geology, 51*, 136–151. https://doi.org/10.1016/j.marpetgeo.2013.12.004

Henares, S., Caracciolo, L., Viseras, C., Fernández, J., and Yeste, L. M. (2016). Diagenetic constraints on heterogeneous reservoir quality assessment: A Triassic outcrop analog of meandering fluvial reservoirs. *AAPG Bulletin, 100*(9), 1377–1398. https://doi.org/10.1306/04041615103

Howell, J., and Mountney, N. (2001). Aeolian grain flow architecture: hard data for reservoir models and implications for red bed sequence stratigraphy. *Petroleum Geoscience, 7*(1), 51–56. https://doi.org/10.1144/petgeo.7.1.51

Howell, J. A., Schwarz, E., Spalletti, L. A., and Veiga, G. D. (2005). The Neuquén basin: an overview. In G. D. Veiga, L. A. Spalletti, J. A. Howell, E. Schwarz (Eds.), *The Neuquén Basin, Argentina: A Case Study in Sequence Stratigraphy and Basin Dynamics*, Geological Society, London, Special Publications, 252(1), 1–14. https://doi.org/10.1144/GSL.SP.2005.252.01.01

Huang, Y., Ringrose, P. S., and Sorbie, K. S. (1995). Capillary trapping mechanisms in water-wet laminated rocks. *SPE Reservoir Engineering, 10*(04), 287–292. https://doi.org/10.2118/28942-PA

Huang, Y., Ringrose, P. S., Sorbie, K. S., and Larter, S. R. (1996). The effects of heterogeneity and wettability on oil recovery from laminated sedimentary structures. *SPE Journal, 1*(04), 451–462. https://doi.org/10.2118/30781-PA

Hunter, R. E. (1977). Basic types of stratification in small eolian dunes. *Sedimentology, 24*(3), 361–387. https://doi.org/10.1111/j.1365-3091.1977.tb00128.x

Hunter, R. E. (1985). Subaqueous sand-flow cross strata. *Journal of Sedimentary Research, 55*(6), 886–894. https://doi.org/10.1306/212F8832-2B24-11D7-8648000102C1865D

Hunter, R. E., and Kocurek, G. (1986). An experimental study of subaquaeous slipface deposition. *Journal of Sedimentary Research, 56*(3), 387–394. https://doi.org/10.1306/212F8922-2B24-11D7-8648000102C1865D

Jarzyna, J., Puskarczyk, E., Bała, M., and Papiernik, B. (2009). Variability of the Rotliegend sandstones in the Polish part of the Southern Permian Basin-permeability and porosity relationships. *Annales Societatis Geologorum Poloniae 79*(1), 13–26.

Kahn, J. S. (1956). The analysis and distribution of the properties of packing in sand-size sediments: 1. On the measurement of packing in sandstones. *The Journal of Geology, 64*(4), 385–395. https://doi.org/10.1086/626372

Kocurek, G., and Dott, R. H. (1981). Distinctions and uses of stratification types in the interpretation of eolian sand. *Journal of Sedimentary Research, 51*(2), 579–595. https://doi.org/10.1306/212F7CE3-2B24-11D7-8648000102C1865D

Legarreta, L., and Gulisano, C. A. (1989). Análisis estratigráfico secuencial de la Cuenca Neuquina (Triásico superior-Terciario inferior). *Cuencas sedimentarias argentinas, 6*(10), 221–243. 10° Congreso Geológico Argentino.

Legarreta, L., and Uliana, M. A. (1991). Jurassic—marine oscillations and geometry of Back-arc basin fill, central Argentine Andes. In D. I. M. Macdonald (Ed.), *Sedimentation, Tectonics and Eustasy: Sea-Level Changes at Active Margins*, 429–450. Wiley. https://doi.org/10.1002/9781444303896.ch23

Limarino, C. O., Spalletti, L. A., and Piñol, F. C. (2015). Microfabrics in eolian sandstones of the De La Cuesta Formation (Permian), Sierra de Narváez, Catamarca Province, Argentina. *Latin American Journal of Sedimentology and Basin Analysis, 22*(2), 83–108. https://lajsba.sedimentologia.org.ar/lajsba/article/view/194

Limarino, C. O, Marenssi, S. A., and Ciccioli, P. L. (2025). *Petrología de areniscas y conglomerados.*

Mountney, N. P. (2006) Eolian Facies Models. In H. Posamentier and R. G. Walker (Eds.), *Facies Models Revisited*, SEPM Society for Sedimentary Geology 84, 19–83. https://doi.org/10.2110/pec.06.84.0019

Nichols, G. (2009). *Sedimentology and stratigraphy* (2nd ed.). Wiley-Blackwell.

Nickling, W. G., Neuman, C. M., and Lancaster, N. (2002). Grainfall processes in the lee of transverse dunes, Silver Peak, Nevada. *Sedimentology, 49*(1), 191–209. https://doi.org/10.1046/j.1365-3091.2002.00443.x

Pandalai, H. S., and Basumallick, S. (1984). Packing in a clastic sediment: concept and measures. *Sedimentary geology, 39*(1–2), 87–93. https://doi.org/10.1016/0037-0738(84)90027-7

Pickup, G. E., Ringrose, P. S., Corbett, P. W. M., Jensen, J. L., and Sorbie, K. S. (1994). Geology, geometry, and effective flow. *Petroleum Geoscience 1* (1), 37–42. https://doi.org/10.1144/petgeo.1.1.37

Prámparo, M. B., and Veiga, G. D. (2024). Palynological data from the Hauterivian Avilé Member, Pampa Tril section, Agrio Formation, Neuquén Basin, Argentina. *Journal of South American Earth Sciences, 138*, 104865. https://doi.org/10.1016/j.jsames.2024.104865

Pringle, J. K., Howell, J. A., Hodgetts, D., Westerman, A. R., and Hodgson, D. M. (2006). Virtual outcrop models of petroleum reservoir analogues: a review of the current state-of-the-art. *First break, 24*(3). https://doi.org/10.3997/1365-2397.2006005

Robinson, A. E. (1981). *Facies types and reservoir quality of the Rotliegendes Sandstone, North Sea*. [abstract]. 1981 SPE Annual Technical Conference and Exhibition, San Antonio, Texas. https://doi.org/10.2118/10303-MS

Rodríguez-López, J. P., Clemmensen, L. B., Lancaster, N., Mountney, N. P., and Veiga, G. D. (2014). Archean to Recent aeolian sand systems and their sedimentary record: current understanding and future prospects. *Sedimentology, 61*(6), 1487–1534. https://doi.org/10.1111/sed.12123

Roduit, N. (2022). JMicroVision (Version 1.3.4) [Computer software]. Geneva, Switzerland: N. Roduit. https://jmicrovision.github.io.

Rosenfeld, M. A., Jacobsen, L., and Ferm, J. C. (1953). A comparison of sieve and thin-section technique for size analysis. *The Journal of Geology, 61*(2), 114–132. https://doi.org/10.1086/626060

Rossi, G. and Masarik, C. 2002. Acumulaciones de hidrocarburos en areniscas eólicas. Un ejemplo del hauteriviano de la Cuenca Neuquina. 15º Congreso de Exploración de Hidrocarburos, Mar del Plata.

Scasso, R. A., and Limarino, C. O. (1997). *Petrología y diagénesis de rocas clásticas*. Publicación Especial 1, Asociación Argentina de Sedimentología.

Schenk, C. J. (1983). Textural and structural characteristics of some experimentally formed eolian strata. In M.E. Brookfield and T.S. Ahlbrandt (Eds.), *Eolian Sediments and Processes*, Developments in Sedimentology, 38, 41–49. https://doi.org/10.1016/S0070-4571(08)70787-8

Sharp, R. P. (1963). Wind ripples. *The Journal of Geology, 71*(5), 617–636. https://doi.org/10.1086/626936

Spalletti, L. A., and Veiga, G. D. (2007). Variability of continental depositional systems during lowstand sedimentation: an example from the Kimmeridgian of the Neuquén Basin, Argentina. *Latin American journal of sedimentology and basin analysis, 14*(2), 85–104. https://lajsba.sedimentologia.org.ar/index.php/lajsba/article/view/96

Taylor, J. M. (1950). Pore-space reduction in sandstones. *AAPG Bulletin, 34*(4), 701–716. https://doi.org/10.1306/3D933F47-16B1-11D7-8645000102C1865D

The MathWorks, Inc. (2022). MATLAB (Version 9.13.0, R2022b) [Computer software]. Natick, Massachusetts: The MathWorks, Inc. https://www.mathworks.com

Tucker, Maurice E. (2001). *Sedimentary petrology: An introduction to the origin of sedimentary rocks* (3rd ed.). Blackwell Science.

Tucker, M. E., and Jones, S. J. (2023). *Sedimentary petrology*. John Wiley and Sons.

Valenzuela, M., Schiuma, M., Hinterwimmer, G., and Vergani, G. (2002). Los reservorios del Miembro Avilé de la Formación Agrio. *Rocas Reservorio de las Cuencas Productivas de la Argentina*, 5º Congreso de Exploración y Desarrollo de Hidrocarburos, 433–446.

Valenzuela, M. E., Cómeron, R., Masarik, M. C., and Vallejo, M. D. (2011). Yacimientos Chihuido de la Sierra Negra, Lomita, Lomita Norte y El Trapial. In H. A. Leanza, C. Arregui, O. Carbone, D. N. Danieli, and J. C. Vallés (Eds.), *Geología y Recursos Naturales de la Provincia del Neuquén*, Relatorio del XVIII Congreso Geológico Argentino, 677–688. Asociación Geológica Argentina.

Veiga, G. D., Spalletti, L. A., and Flint, S. (2002). Aeolian/fluvial interactions and high-resolution sequence stratigraphy of a non-marine lowstand wedge: the Avilé Member of the Agrio Formation (Lower Cretaceous), central Neuquén Basin, Argentina. *Sedimentology, 49*(5), 1001 –1019. https://doi.org/10.1046/j.1365-3091.2002.00487.x

Veiga, G. D., Spalletti, L. A., and Flint, S. (2007). Anatomy of a fluvial lowstand wedge: the Avilé Member of the Agrio Formation (Hauterivian) in central Neuquén Basin (northwest Neuquén province), Argentina. In G. Nichols, E. Williams, and C. Paola (Eds.), *Sedimentary Processes, Environments and Basins: A Tribute to Peter Friend*, 341–365. https://doi.org/10.1002/9781444304411.ch16

Veiga, G. D., Spalletti, L. A., and Schwarz, E. (2011). El Miembro Avilé de la Formación Agrio (Cretácico Temprano). In H. A. Leanza, C. Arregui, O. Carbone, D. N. Danieli, and J. C. Vallés (Eds.), *Geología y Recursos Naturales de la Provincia del Neuquén*, Relatorio del XVIII Congreso Geológico Argentino, 2–6. Asociación Geológica Argentina.

Vergani, G. D., Tankard, A. J., Belotti, H. J., and Welsink, H. J. (1995). Tectonic evolution and paleogeography of the Neuquén Basin, Argentina. In A. J. Tankard, R. Suárez Soruco, and H. J. Welsink (Eds.), *Petroleum basins of South America*, American Association of Petroleum Geologists, 383–402. https://doi.org/10.1306/M62593C19

Visher, G.S. (1969) Grain-Size Distribution and Depositional Processes. *Journal of Sedimentary Petrology, 39*, 1074–1106